TRIPLE-NEGATIVE BREAST CANCER STEM CELL MARKER ALDH1A3 REGULATES THE PLASMINOGEN PATHWAY TO PROMOTE INVASION AND METASTASIS

by

Meghan McLean

Submitted in partial fulfilment of the requirements
for the degree of Master of Science

at

Dalhousie University
Halifax, Nova Scotia
September 2023

Dedication Page

I dedicate this work to my uncle, Tim Graves. You drove my passion for cancer research and kept the flame of determination alive within me when no one else could. Live, love, laugh.

Table of contents

List of Tables

List of Figures

Abstract

Aldehyde dehydrogenase 1A3 (ALDH1A3) is a cancer stem cell marker that also increases tumour growth, promotes metastasis, and contributes to chemoresistance. Metastasis of triple-negative breast cancer (TNBC) has been linked to gene expression changes induced by ALDH1A3. To investigate the mechanism of ALDH1A3-mediated breast cancer metastasis, we assessed the effect of ALDH1A3 on the expression of proteases and the regulators of proteases that degrade the extracellular matrix, which is essential for invasion and metastasis. This revealed that ALDH1A3 regulates the plasminogen activation pathway; it increased the levels and activity of tissue plasminogen activator (tPA) and urokinase plasminogen activator (uPA). This resulted in a corresponding increase in the activity of serine protease plasmin, the enzymatic product of tPA and uPA. All-trans-retinoic acid, which is produced by ALDH1A3 and is a hormone receptor ligand, similarly led to an increased tPA and plasmin activity. DNA methylation also regulates tPA at the gene level where CpG methylation near the transcription start site prevents expression of tPA. Increased invasion of TNBC cells by ALDH1A3 was plasminogen-dependent. In patient tumours, ALDH1A3 and tPA are co-expressed and their combined expression correlated with the TNBC subtype, high tumour grade, and recurrent metastatic disease. Knockdown of tPA in TNBC cells inhibited plasmin generation, invasion, and lymph node metastasis. These results identify the ALDH1A3-tPA-plasmin axis as a key contributor to breast cancer progression.

List of Abbreviations and Symbols Used

ADAM	Disintegrin and metalloprotease
ADAMTS	Disintegrin and metalloprotease with thrombospondin motif
ALDH	Aldehyde dehydrogenase
ALDH1A3	Aldehyde dehydrogenase 1A3
ALDH^{high}	Aldefluor-positive
ATRA	All-trans retinoic acid
CSC	Cancer stem cell
CXCR4	C-X-C chemokine receptor type 4
DCIS	Ductal carcinoma in situ
DEAB	Diethylaminobenzaldehyde
ECM	Extracellular matrix
EMT	Epithelial-to-mesenchymal transition
EpCAM	Epithelial cell adhesion molecule
ER	Estrogen receptor
FBS	Fetal Bovine Serum
GABA	Gamma-aminobutyric acid
GAPDH	Glyceraldehyde 3-phosphate dehydrogenase
HAT	Histone acetylases
HDAC	Histone deacetylase
HER2	Human epidermal growth factor 2
HOXA1	Homeobox A1

HUVEC	Human umbilical vein epithelial cell
IDC	Invasive ductal carcinoma
ILC	Invasive lobular carcinoma
LCIS	Lobular carcinoma in situ
METABRIC	Molecular Taxonomy of Breast Cancer International Consortium
MMP	Matrix metalloproteinases
MUC4	Mucin 4
NAD^+	Nicotinamide adenine dinucleotide
$NADP^+$	Nicotinamide adenine dinucleotide phosphate
NOD-SCID	Nonobese diabetic/severe combined immunodeficiency
PAI-1	Plasminogen-activator-inhibitor 1
PAI-2	Plasminogen-activator-inhibitor 2
PDE5	type 5 phosphodiesterase
pNA	*p*-nitroanilide
PR	Progesterone receptor
PRC2	Polycomb repressive complex 2
PVDF	polyvinylidene difluoride
QEII HSC	Queen Elizabeth II Health Science Center
qPCR	Quantitative polymerase chain reaction
RA	Retinoic acid
RALDH1	Retinal dehydrogenase 1
RAR	Retinoic acid receptor

RARE	Retinoic acid receptor element
RNA-seq	RNA sequencing
RT-qPCR	reverse-transcription quantitative PCR
RXR	Retinoid X receptor
SDS-PAGE	Sodium dodecyl-sulfate polyacrylamide gel electrophoresis
SF-CM	Serum-free conditioned media
shRNA	short hairpin RNA
STR	Short-term repeat profiling
TCGA	The Cancer Genome Atlas Program
TIMP3	Tissue inhibitor of metalloproteinase 3
TMPRSS3	Transmembrane serine proteases 2
TNBC	Triple-negative breast cancer
tPA	Tissue plasminogen activator
TTS	Transcription start site
uPA	Urokinase plasminogen activator
uPAR	Urokinase plasminogen activator receptor

Acknowledgements

First and foremost, I would like to thank Dr. Paola Marcato for believing in me during my entire degree. Your motivation and positive attitude drove me to reach my potential. Our morning chats, elaborate discussions and high-fives always left me feeling like I could take on the world. I will truly forever look up to you and I was honoured to be a part of your lab.

Dr. Alamelu Bharadwaj, thank you for providing mentorship and warm smiles. You showed me where hard work can take you. Your drive for science inspires me, and I could not have asked for a better collaborator to complete a paper with. I would also like to thank Lynn Thomas for always greeting me like a ray of sunshine. Your kind words and Christmas cookies will always be remembered.

To my lab mates who made coming to the lab such a joy, I thank all of you for providing unlimited laughter. The friendships that we have made will be cherished forever and I am so proud of how much we have accomplished together. Life was meant for good friends and great adventures, and I can't wait to see where success takes us all.

I would also like to thank my family and friends. To my parents, thank you for your unconditional love and support. Throughout my schooling, you have always guided me to be my best and obtaining an MSc would never have been possible without you. Finally, I would like to acknowledge George Ridgeway. Your unwavering belief in me and consistent encouragement have been a source of strength and inspiration.

Chapter 1 Introduction

1.1 Cancer

Cancer is an ancient disease that has made its mark by negatively affecting human health around the world[1]. The earliest evidence of human cancer was found in an ancient Egyptian manuscript, dating back to 1500 BC[2]. During this time, the development of cancer in an individual was not understood and surgery was the main treatment to remove the tumour. In the 18th century, it was discovered that cancer cells were derived from healthy cells within the individual and not from an imbalance of fluids in the body as previously believed[3,4]. This finding provided an alternate explanation to the belief that cancer cells arose from chronic irritation, trauma, or parasites. In the middle of the 20th century, Watson and Crick's discovery of the DNA helix ultimately led to the profound realization that cancer is a genetic disease[5]. Today, many research groups all over the world are dedicated to bettering the understanding of the genetic components of cancer to identify novel strategies to combat the disease.

In the genome, the acquisition of mutations can result in the transformation of a normal cell to a cancer cell. The type of gene in which the mutation occurs influences the phenotypic outcome of this error. In the context of cancer, there are two types of genes in which mutations are often studied: oncogenes and tumour-suppression genes. Oncogenes become amplified or constitutively activated by mutations allowing cancer cells to divide uncontrollably, proliferate, resist cell death, and promote cell survival[6]. In normal cells, these genes are tightly regulated; however, certain mutations in cancer cells will "turn on" oncogenes uncontrollably to promote cancer. In contrast to oncogenes, tumour suppressors are genes that become silenced, leading to pro-tumourigenic properties[7]. In normal cells, these genes are present to ensure the cell has appropriate controls in place to prevent cells with damaged DNA from dividing and repair DNA

damage. Mutations in cancer cells can "turn off" these genes, therefore allowing DNA-damaged cells to avoid apoptosis and to continue to replicate. The faulty DNA repair pathways in these cancer cells can result in the acquisition of additional mutations leading to alterations of gene expression which can promote tumourigenic pathways. Ultimately, the accumulation of mutations allows cancer cells to gain the ability to spread beyond their primary tumour site and contribute to cancer progression by enabling invasion and metastasis.

Invasion is the process by which cancer cells migrate to nearby environments[8]. To do this, cancer cells break down important components of the extracellular matrix (ECM) to permit growth into neighbouring or distant tissue. The components of the ECM, including collagen, elastin and fibrin, are enzymatically degraded by proteases, thereby facilitating invasion [9]. For example, matrix metalloproteinases (MMPs) degrade fibrin and collogen in the ECM in many cancer types[10]. Invasion is an important hallmark of cancer, as this process helps to initiate metastasis[11].

Cancer cell metastasis can be enabled by the epithelial-to-mesenchymal transition (EMT) [12]. During this transition, cancer cells downregulate attachment proteins, such as e-cadherin, to detach from neighbouring cells [13]. This loss of e-cadherin permits cancer cells to migrate away from their primary tumour site, allowing for potential tumour spread and growth in different parts of the body. As metastasis is the primary cause of patient death [14], further research is needed to understand the mechanisms that drive this process, so that patient health and survival can be improved.

Aberrant expression of genes promote cancer cell invasion and metastasis, creating a complex disease which affects individuals worldwide. In Canada, 2 of 5 individuals will be diagnosed with cancer at some point in their life[15], with lung, breast, colorectal and prostate

cancers among the most diagnosed cancer types. Of these diagnosed individuals, 1 out of 4 will succumb to the disease. The immense number of individuals affected by this disease demonstrates the importance of studying the molecular factors that drive cancer, especially those contributing to cancer metastasis so that new treatments can be found to improve patient survival.

1.2 Breast Cancer

In women, breast cancer is the most diagnosed cancer type, making up 37.1% of cancer cases[15]. Furthermore, breast cancer mortality poses a substantial concern, as 13% of cancer deaths in women are due to breast cancer according to the Canadian Cancer Society. Fortunately, breast cancer research has advanced in the last decade, resulting in improved screening and diagnoses, which have translated to better outcomes for many breast cancer patients.

Breast cancer can be classified based on histological and morphological sub-types. There are four main types of breast cancer: invasive ductal carcinoma (IDC), ductal carcinoma in situ (DCIS), invasive lobular carcinoma (ILC), and lobular carcinoma in situ (LCIS)[16]. As the names suggest, IDC and DCIS form in the lining of the milk ducts whereas ILC and LCIS form in the milk lobules in the breast tissue. While DCIS and LCIS are considered cancerous, they are non-invasive tumours that reside within the ducts and lobules, respectively. In contrast, IDC and ILC are invasive cancers that have spread into surrounding tissues. If untreated, DCIS and LCIS have the potential to turn into IDC and ILC respectively, but histological assessment on its own cannot predict if this will occur. Out of these four types, IDC is the most diagnosed form of breast cancer [17].

Besides histological assessments, breast cancer is also classed by receptor subtypes. The receptors are the estrogen receptor (ER), progesterone receptor (PR) and/or human epidermal

growth factor 2 (HER2) receptor[18]. The breast cancer subtype is determined to be receptor-positive or negative based on the presence of these receptors. When all three receptors are absent, the breast cancer is classified as triple-negative breast cancer (TNBC). The breast cancer subtype dictates the therapeutic strategy used, the presence or lack of receptors therefore plays a major role in guiding treatment decisions[19].

For hormone-positive breast cancers, hormone therapy drugs can be used to block estrogen and progestogen receptors to prevent cells from receiving signals from these hormones[20]. This inhibits the growth of cancer cells due to their inability to survive without these hormones. In HER2-positive breast cancers, monoclonal antibodies have been created to block the HER2 receptor and therefore prevent cell growth[21]. These types of therapies have shown to be successful and have led to better prognoses for many breast cancer patients. For TNBC, neither hormone therapy nor HER2 monoclonal antibodies help fight the disease as TNBCs do not present the receptors. Unfortunately for TNBC patients, chemotherapy is the main treatment option despite its high resistance rate [22].

Among the breast cancer subtypes, TNBC is the most aggressive and has the worst patient survival outcomes[23]. TNBC makes up 10-15% of all breast cancer and is more commonly diagnosed in women under the age of 40 and in black women[24]. Understanding the molecular factors that drive TNBC metastasis can lead to advances in treatment options and better patient outcomes. One of these factors is aldehyde dehydrogenase 1A3 (ALDH1A3).

Contributions statement

I conducted a comprehensive literature review on the latest research pertaining to ALDH1A3 in cancer and other diseases. Subsequently, I systematically organized the relevant papers into distinct sections, elucidating ALDH1A3's multifaceted roles in cancer, patient prognosis, underlying mechanisms, and potential therapeutic inhibitors. Collaborating with my laboratory colleagues, we further enriched these topics to enhance the understanding of ALDH1A3's significance.

Meghan McLean: Conceptualization, Writing—Original Draft, Writing—Review and Editing. **Maya MacLean**: Writing—Original Draft, Writing—Review and Editing. **Hannah Cahill**: Writing—Original Draft, Writing—Review and Editing. **Olivia Walker**: Writing—Original Draft, Writing—Review and Editing. **Raj Arun Pranap**: Writing—Original Draft, Writing—Review and Editing. **Marie-Claire Wasson**: Writing—Original Draft, Writing—Review and Editing. **Wasundara Fernando**: Writing—Original Draft, Writing—Review and Editing. **Jaganathan Venkatesh**: Writing—Original Draft, Writing—Review and Editing. **Paola Marcato**: Conceptualization, Supervision, Writing—Original Draft, Review and Editing, Project administration. All authors have read and agreed to the published version of the manuscript.

1.3 ALDH1A3

Found to be generally expressed at low levels in the body, with higher amounts in the salivary gland, stomach, and kidneys, ALDH1A3 was the sixth ALDH enzyme discovered in the human genome and was initially called ALDH6[25]. Eventually, 19 ALDH enzymes expressed from the distinct genetic loci in the human genome were discovered. The 19 members comprise the ALDH superfamily and share at least 40% sequence homology, with subfamily members sharing at least 60% homology[26,27].

ALDHs catalyze the irreversible oxidation of aldehydes to carboxylic acids by binding an aldehyde and cofactor nicotinamide adenine dinucleotide (NAD^+) or NAD phosphate ($NADP^+$). In general, ALDHs function to remove toxic aldehydes generated during metabolic processes including endogenous aldehydes that arise from lipid peroxidation, amino acid catabolism and exogenous xenobiotics[27]. In addition, the isoforms have distinct expression profiles in body tissues, differing subcellular locations (cytoplasm, nucleus, endoplasmic reticulum, or mitochondria), substrate specificity, and function. Pertinent to this review, the homologous ALDH1A1, ALDH1A2, and ALDH1A3 isoforms share 70% amino acid sequence homology, are

cytoplasmic, and oxidize the vitamin A metabolite all-trans retinal to all-trans retinoic acid (ATRA, also commonly referred to as retinoic acid, RA). Due to this retinal oxidizing activity, ALDH1A1, ALDH1A2, and ALDH1A3 are also called retinal dehydrogenase 1 (RALDH1), RALDH2, and RALDH3, respectively.

The three ALDH1A enzymes have important and distinct roles in embryonic development. ALDH1A3 is expressed in the ventral retina and its loss causes anophthalmia and aberrant eye development in humans and animal models[28–30]. ALDH1A3 knockout in mice is neonatal-lethal, with severe defects in nasal and eye development, due to RA deficiency during critical developmental periods [31].

A comparative analysis of the three ALDH1A enzymes revealed similar structural topologies, with ALDH1A3 having the smallest substrate-binding pocket[31]. ALDH1A3 had the highest enzymatic activity for the conversion of all-trans-retinal to RA, followed by ALDH1A2, but comparatively had the least activity with other tested substrates[31]. This was consistent with earlier reports suggesting the greater RA biosynthetic capacity of ALDH1A3 over ALDH1A1[32].

1.4 ALDH1A3 regulates gene expression through retinol acid signalling

RA is a developmentally important cell signalling molecule; it is a ligand for the nuclear hormone receptor retinoic acid receptor (RAR), capable of regulating the expression of hundreds of genes and resulting in diverse cellular effects[27,33–35]. A requisite of RA signaling is that cells can metabolize vitamin A (retinol) to retinal and then retinal to RA.

RA binds to the nuclear hormone receptors retinoic acid (RAR) α, β, γ, which form heterodimers with the retinoid X receptor (RXR)[36]. The heterodimers regulate gene expression by binding to retinoic acid receptor element (RARE) sequence motifs found in the promoters and

enhancer regions of over 3000 genes in the genome[37]. The binding of RA to these heterodimer nuclear hormone receptors can have both activating and repressing gene expression effects. Gene induction is observed when RA binding to RAR promotes the binding of co-activators of the nuclear receptors and other co-activators such as histone acetylases (HATs). Inversely, in a mechanism that is less understood, gene repression by RA involves RA-mediated recruitment of polycomb repressive complex 2 (PRC2) and superfamily histone deacetylase (HDAC) to nuclear hormone receptor heterodimers.

RA signalling in the physiological range (nM amounts) is mediated by the ALDH1A enzymes and has distinct effects from the supra-physiological effects induced by pharmacological RA treatment, which is in the μM range. Supra-physiological amounts of RA can inhibit cell proliferation and induce cell death and differentiation as seen in the treatment of acute promyelocytic leukemia[38–40]. RA treatment can reduce the severity of asthma[41,42], while in contrast retinoid and vitamin A deficiency exacerbates the condition[43,44]. Gene expression analysis indicated elevated ALDH1A3 expression in asthma patients[45]; however, another study showed no change in ALDH1A3 protein expression levels[42].

Overall, these studies suggest that in the context of cancer and other illnesses, pharmacological retinoid treatment effects often differ from ALDH1A-mediated physiological RA signalling and the two should not be necessarily equated.

1.5 ALDH1A3 is a cancer stem cell marker

Cancer stem cells (CSCs) are a small subpopulation of cells within tumours that exhibit characteristics of both stem cells and cancer cells. CSCs are enriched for various markers, with some cancer-type specificity. These markers include cell surface markers like CD133, CD24,

CD44, and epithelial cell adhesion molecule (EpCAM)[46]. Among the most common methods to identify cancer cell populations enriched for CSCs is increased ALDH activity detected by the Aldefluor assay[47]. Aldefluor-positive (also referred to as $ALDH^{bright\ or}$ $ALDH^{high}$) populations were initially identified as having CSC qualities (i.e., having increased tumourigenicity and giving rise to heterogeneous tumours) in murine xenograft studies with breast cancer by Ginestier *et. al*,[48] and leukaemia by Cheung *et.al,* [49]. Aldefluor-positive-isolated cancer cells have been similarly shown to generate xenograft tumours with high efficiency in the liver, head and neck, lung, pancreatic, cervical, thyroid, prostate, colon, bladder, and ovarian cancers[50–58].

The Aldefluor assay measures the conversion of ALDH substrate, BODIPY™ amino acetaldehyde to fluorescent reaction product BODIPY™ aminoacetate. The addition of inhibitor diethylaminobenzaldehyde (DEAB) reduces fluorescence, confirming that Aldefluor-positive cells are correctly identified. This assay was originally developed for the isolation of viable hematopoietic stem cells from human umbilical cord blood[59] and was initially believed to be specific for one ALDH isoform found in high abundance in those cells: ALDH1A1. Therefore, Aldefluor-positive cells are sometimes referred to as ALDH1 positive or ALDH1A1 positive. This can be a wrong assumption since the BIODIPY aminoactealdehyde substrate is not specific to ALDH1A1 and other ALDH enzymes can generate the fluorescent product if expressed in sufficient levels[47].

Multiple studies have demonstrated that ALDH1A3 is an ALDH isoform that is at least as important as ALDH1A1 in influencing the Aldefluor activity of cancer cells. For breast cancer, gene expression analysis and knockdown of the 19 ALDH isoforms revealed that ALDH1A3 expression was the primary isoform contributing to Aldefluor activity of breast cancer patient tumours and cell lines[60]. Later, similar studies performed in melanoma cancer implicated both

ALDH1A1 and ALDH1A3 expression as being important in determining Aldefluor activity and CSC activity[61]. Similarly, in mesenchymal glioma stem cells, Aldefluor-positivity was associated with enriched ALDH1A3 expression and stemness[62]. Profiling the ALDH isoforms by gene expression and knockdown in non-small cell lung cancer similarly revealed the importance of ALDH1A3 in the Aldefluor activity of cancer and tumourigenicity[63]. In colon cancer, analysis of expression and knockdown of the 19 ALDH isoforms in 58 cell lines again suggested the primary importance of ALDH1A3 in the Aldefluor activity colon[64]. In intrahepatic cholangiocarcinoma (bile duct cancer) ALDH1A3 was found the main contributor to Aldefluor activity[65]. In head and neck cancer, ALDH activity and stemness were associated with ALDH1A3 expression[66]. ALDH1A3 imparts stemness, tumourigenicity, and Aldefluor activity in gastric cancer[67]. In addition to highlighting the role of ALDH1A3 in the Aldefluor activity of multiple cancers, these studies also demonstrate that when identifying CSCs, detecting the expression of ALDH enzymes is not equal to performing the Aldefluor assay[68].

It is important to note that ALDH1A3 is also commonly measured by many other methods, including immunohistochemistry and immunofluorescence, western blotting, RNA sequencing, and quantitative polymerase chain reaction (QPCR). Many of the subsequent studies we discuss detect and quantify ALDH1A3 in cells and tissues by these other methods.

1.6 ALDH1A3 is associated with worse prognosis in cancer

Consistent with ALDH1A3's association with CSCs, ALDH1A3 expression in cancer is generally associated with worse outcomes, progressive disease, and recurrence. In breast cancer, patient tumours with high levels of ALDH1A3 were associated with an increased incidence of metastasis compared to those with low levels of ALDH1A3[60]. ALDH1A3 is higher in triple-

negative breast cancer (TNBCs), which is an aggressive subtype of breast cancer[69]. In TNBC, ALDH1A3 is associated with worse survival. In addition, high ALDH1A3 expression is associated with worse patient survival in prostate, glioblastoma, neuroblastoma, pancreatic, gastric, gall bladder, colon, and intrahepatic cholangiocarcinoma cancers[65,69–76]. High levels of ALDH1A3 are correlated with increased tumour grade in breast, glioblastoma, bladder, and prostate cancer[69–71,77]. Bladder cancer, breast cancer, and intrahepatic cholangiocarcinoma were shown to have increased ALDH1A3 expression along with high tumour stage[65,69,77].

Although ALDH1A3 is associated with increased tumour progression and worse prognosis in many cancer types, increased ALDH1A3 expression has also been associated with better patient outcomes in TP53 wildtype ovarian tumours, BRAF-mutated metastatic melanoma, and non-small cell lung cancer[63,78,79]. These positive clinical correlates with ALDH1A3 in a different context suggest that ALDH1A3 effects in cancer could be cellular context-specific and dependent on the presence of other molecular factors.

1.7 ALDH1A3 promotes tumour progression

The association of ALDH1A3 with CSCs in multiple cancers implies its importance to cancer progression and aggressiveness. Indeed, ALDH1A3 can facilitate cancer progression by promoting tumour growth and metastasis, and these effects are mirrored *in vitro* assays across multiple cancers.

Knockdown of ALDH1A3 inhibited the growth of the glioma Aldefluor-positive cells, suggesting that ALDH1A3 contributes to CSC-mediated tumourigenicity of mesenchymal glioma[62]. In melanoma cells, ALDH1A3 knockdown reduced tumour growth activity[61]. In non-small cell lung cancer, tumourigenicity was reduced upon ALDH1A3 knockdown[63]. In

breast cancer, the effects of ALDH1A3 were not as clear, with ALDH1A3 promoting tumour growth in two TNBC cell lines (MDA-MB-231 and MDA-MB-435 cells) but inhibiting in a third (MDA-MB-468 cells)[69]. The mechanism behind this discrepancy may be related to cell line-specific differential epigenetic-silencing of key ALDH1A3-inducible genes, including mucin 4 (MUC4) and homeobox A1 (HOXA1). In gastric cancer, ALDH1A3 knockdown reduced tumour growth[75]. In osteosarcoma, tumourigenicity was associated with ALDH1A3 expression[80].

ALDH1A3 also contributes to metastasis. In TNBC MDA-MB-231 cells increased ALDH1A3 resulted in a corresponding increase in lung metastasis in the orthotopic xenograft model[69]. Knockdown of ALDH1A3 in HPAC pancreatic cancer cells reduced lung metastasis using tail vein injections[76]. ALDH1A3 has been linked to pancreatic cancer metastasis.

In vitro, analyses suggest that ALDH1A3 effects on tumour growth and metastasis are multifactorial. ALDH1A3 knockdown melanoma cell lines resulted in decreased cell proliferation and increased apoptosis [61,81]. In colon cancer cell lines, ALDH1A3 knockdown decreased cell proliferation and C-X-C chemokine receptor type 4 (CXCR4) expression, suggesting a potential connection between the two[64]. In lung cancer cell lines, reduced ALDH1A3 expression was associated with decreased cell proliferation[82]. In gastric cancer cells, ALDH1A3 knockdown reduced cell proliferation[75].

Although the increased metastasis associated with increased ALDH1A3 could be an indirect result of increased tumour burden and cancer cell proliferation, there is also evidence that ALDH1A3 directly increases the metastatic potential of a cancer cell. There are many reports of ALDH1A3 affecting invasion and/or migration, but these effects appear cancer-type dependent. For breast cancer, increased ALDH1A3 results in increased transwell invasion of TNBC MDA-MB-231 cells[69]. The increased invasion/metastatic potential imparted by ALDH1A3 on breast

cancer cells appears connected to decreased migration. ALDH1A3 knockdown in TNBC MDA-MB-468 and SUM159 cells increased adhesion and migration while decreasing metastasis in a chick chorioallantoic membrane assay[83]. ALDH1A3 knockdown in cholangiocarcinoma bile duct cancer cell lines decreases migration[65].

Reports also suggest that ALDH1A3 imparts increased colony formation or clonogenicity, which measures the ability of a single cell to form a colony, an *in vitro* indicator of tumour-initiating capacity, required to form primary and secondary tumours [84]. In a panel of lung cancer cell lines, ALDH1A3 knockdown reduced colony formation in 11 out of 12 cell lines[63]. In breast cancer, ALDH1A3 imparted increased colony formation to TNBC MDA-MB-231 and MDA-MB-468 cells[85]. Similarly, in colon and gastric cancers, reduced ALDH1A3 resulted in decreased colony formation[75,86]. In neuroblastoma, ALDH1A3 knockdown reduced clonogenicity[72].

In summary, ALDH1A3 promotes tumour progression, likely via effects on proliferation, apoptosis, migration, invasion, and clonogenicity. The accumulating evidence of ALDH1A3 as a key factor in cancer progression across multiple cancer types suggests it is a promising therapeutic target. It remains unclear what factors ALDH1A3 is regulating to mediate invasion and how it remodels the extracellular matrix.

1.8 Proteases that mediate invasion of cancer cells

To understand ALDH1A3's role in breast cancer invasion and metastasis, we need to first study the mechanisms that drive it. For cancer cells to invade, ECM remodelling takes place. Proteases degrade the ECM promoting remodelling and cancer cell invasion[87]. Furthermore, many cancer types have shown a strong positive correlation between aggressive tumours and protease expression[88]. In humans, there are 569 known proteases, but only a portion of these have been linked to having cancerous effects[89]. Among these cancer-promoting proteases are

disintegrin and metalloproteinases (ADAM), Transmembrane serine proteases 2 (TMPRSS2), plasmin and matrix metalloproteinases (MMPs).

ADAM are membrane-bound proteolytic enzymes that have been shown to promote the degradation of the ECM by shedding growth factors and cytokines[90]. The ADAMs domain influences cell signalling molecules to promote cell invasion. ADAM-17 is a well-studied ADAM domain that has been shown to shed many membrane-bound proteins such as heparin-binding EGF, transforming growth factor-α and E-selectin to promote ECM degradation and invasion[91]. Opposed to being membrane-bound, disintegrin and metalloproteinase with thrombospondin motifs (ADAMTS) are secreted. These ADAMTS proteases can bind and cleave to many different components of the ECM allowing for remodelling and cancer cell invasion[92].

Similar to ADAM, TMPRSS2 is also located on the cell surface. TMPRSS2 consists of intercellular, transmembrane and extracellular domains[93]. The intercellular domain allows for cell signalling pathways to be activated while the extracellular domain has proteolytic activity which can degrade components of the ECM. In prostate cancer, the TMPRSS2 intercellular domain binds to ERG which increases the expression of ETS transcription factor family[94]. This is thought to be an early event in prostate cancer giving rise to many pro-tumourigenic genes.

Plasmin is another important protease in ECM remodelling. Plasmin cleaves fibrin in the ECM and activates pro-MMPs[95–97], accelerating extracellular matrix remodelling required for invasion[98–100]. Plasminogen is a zymogen synthesized and secreted by the liver[101]. The activation of plasminogen to the serine protease plasmin is mediated by activators such as tissue-plasminogen activator (tPA), and the urokinase plasminogen activator (uPA), and its receptor (uPAR). The activation is tightly regulated by the expression of plasminogen-activator-inhibitors (PAI-1 and PAI-2) that inhibit the tPA and uPA activity. In addition, cell surface plasminogen

receptors accelerate the conversion of plasminogen to plasmin by tethering the plasminogen to the cell surface and co-localizing it with its activators[102–104]. The increased ability of the cancer cell to generate plasmin is directly correlated with increased invasive and metastatic potential[105,106]. Plasmin functions in invasion and metastasis by directly degrading the extracellular matrix proteins such as laminin and fibronectin and indirectly by activating MMPs[107].

In normal cells, the plasminogen activation pathway is tightly regulated to help fibrin break down during fibrinolysis[108]. Cancer cells can use this process to their advantage to invade through the ECM. In breast cancer, plasminogen activators tPA and uPA have been shown to increase invasion in vitro. By binding to plasminogen activation receptor annexin II, tPA can induce plasminogen activation in MDA-MB-231 cells which increases invasion[109]. When suppressing annexin II expression, invasion significantly decreased. When looking at uPA expression across different breast cancer cell lines, it was found that when uPA expression was high there was an increase in cell invasion[110]. When antibodies were added to block uPA from binding to the plasminogen activation receptor uPAR, the invasion was decreased.

In terms of plasminogen activator inhibitors, PAI-1 is known for its multifactorial role in breast cancer while PAI-2 remains under studied in vitro. Not only does PAI-1 play a role in uPA and tPA inhibition[111], but it also influences cell proliferation, migration, and apoptosis[112]. Increased PAI-1 stromal expression was also found to correlate with a positive trastuzumab treatment response for HER-2- breast cancer patients[113]. Furthermore, trastuzumab treatment has been shown to be more effective when the uPA receptor is not active[114]. Overall, the plasminogen activating players have been shown to play a role in breast cancer progression, but

understanding the mechanism to drive their expression remains under studied. It is important to understand how proteases are being regulated in cancer for advancement in treatment options.

Proteases in normal cells play a critical role in many cellular processes including cell death, gene expression and differentiation. Cancer cells can use their functions to their advantage and stimulate pro-tumourigenic processes. Protease inhibitors have arisen, however, designing these inhibitors is difficult as different tumours promote different proteases[115]. Therefore, understanding the mechanisms behind protease activation could be a better therapeutic target.

1.9 Targeting ALDH1A3

Targeting CSCs by inhibiting CSC-associated pathways, markers, proteins and non-coding RNAs is a common strategy that is being pursued. For example, the possibility of targeting EpCAM with anti-EpCAM antibodies has been explored extensively and reviewed elsewhere[116]. The Notch signaling pathway, which is commonly activated in CSCs across cancer types, is also a highly explored strategy for targeting CSCs[117]. In particular, γ-secretase inhibitors, which inhibit Notch receptor proteolytic cleavage and signaling, have demonstrated preclinical efficacy with induction of CSC differentiation and apoptosis, inhibition of EMT, and sensitizing to chemotherapies[118]. Targeting non-coding RNAs enriched in CSCs with antisense oligonucleotides has also been suggested as a possibility[79]. The possibility of inhibiting ALDHs and ALDH1A3 specifically in the treatment of cancer and targeting of CSCs has been investigated in recent years by various drugs.

Many compounds have general or semi-specificity for inhibition of ALDH isoforms. These compounds include DEAB, chloral hydrate, citral, coprine, daidzin, gossypol, pargyline, and disulfiram[15]. Disulfiram is an old drug - it has been used to treat alcohol abuse for over 70 years[80]. The liver enzyme alcohol dehydrogenase converts alcohol to acetaldehyde, which then

becomes converted into non-toxic acetic acid by liver ALDH1A1 and ALDH2[80]. Disulfiram inhibition of liver ALDH1A1 and ALDH2 leads to toxic accumulation of acetaldehyde, resulting in an adverse reaction to alcohol consumption that psychologically conditions the patient to associate alcohol with physical pain. Work has been done to repurpose this classic anti-alcoholism drug as a possible treatment for various cancers[81].

As an anti-cancer agent, disulfiram works by several potential mechanisms; in addition to inhibiting ALDHs, it inhibits proteasome function (when complexed with copper; CuET), E3 ligases, and intriguingly may also be a DNA-demethylating agent[82,83]. In terms of inhibiting the ALDH1A3 isoform specifically, disulfiram has minimal ALDH1A3 targeting activity in breast cancer cells[85] and inhibited glioblastoma stem cells independent of effects on ALDH1A3[124]. However, the disulfiram copper complex CuET inhibited colorectal cancer progression by downregulating ALDH1A3 gene expression[86].

Some specificity for ALDH1A3 was observed in citral, where μM concentrations inhibited Aldefluor-mediated ALDH1A3 activity in breast cancer cells and encapsulated citral inhibited ALDH1A3-mediated breast tumour growth[85]. In contrast, the same study showed that diadzin, chloral hydrate, coprine, gossypol, and pargyline did not inhibit ALDH1A3 activity of breast cancer cells even at 100μM concentrations. Interestingly, a modified diadzin analog synthesized to inhibit ALDH1A3 (i.e., imidazo [1,2-*a*] pyridine, G11), had *in vivo* efficacy in a glioblastoma tumour model[125]. In cell-free assays of ALDH1A3 activity, G11 had half maximal inhibitory concentration (IC50) of 22.8μM. A further modification of G11 generated MF-7, which demonstrated improved IC50 in cell free assays (4.7μM)[126]. MC-7 treatment increased the survival of mice in a breast cancer brain metastasis model[126]. The later derived analog NR-6 showed similar anti-cancer activity[127]. More recently, the type 5 phosphodiesterase (PDE5)

inhibitor E4021 was found to bind to ALDH1A3 by protein affinity chromatography approach and sub-μM amounts of derivatized compound ER-001135935 specifically inhibited ALDH1A3 activity *in vitro*[128].

The solving of the crystal structure of ALDH1A3 complexed with NAD+ and ATRA in 2016[129], allows for rationally designed ALDH1A3 specific inhibitors that prevent pocket binding of the substrate binding. This was recently demonstrated by the generation of *in silico*-designed MCI-INI-3, which inhibits ALDH1A3 specifically (IC50 = 0.46μM)[130]. Although not tested yet for anti-cancer activity, this rationally designed inhibitor has the highest specificity and activity among thus far reported ALDH1A3 inhibitors. The crystal structure of ALDH1A3 also allows for the screening of potential ALDH1A3 inhibitors among library compounds by molecular docking modeling. These *in silico* analyses identified YD1701 (dibenzo-30-crown10-ether), as an ALDH1A3 inhibitor[131]. It has a reported IC50 of 12.0824μg/mL (which is equivalent to 22.5μM based on a molecular weight of 536.63 g/mol). YD1701 inhibited the invasion of colon cancer cells and prolonged the survival of mice implanted with colon cancer xenografts.

Likely, if the clinical use of targeting ALDH1A3 is to be realized, it will be in combination with chemotherapies, immunotherapies, and other adjuvant therapies. Potential combination strategies also include inhibiting ALDH1A3 alongside other drugs that target different CSC markers and pathways to limit the emergence of therapy-resistant CSCs.

1.10 Hypothesis and Objectives

Ultimately, I aim to unravel ALDH1A3's mechanism of TNBC metastasis. We hypothesize that ALDH1A3 mediate invasion and metastasis by regulating protease genes or the genes that regulate proteases.

Objective 1: Identify protease genes regulated by ALDH1A3 in TNBC cells

Objective 2: Determine if ALDH1A3 correlates with the expression of these proteases in patient tumour samples

Objective 3: Test if these ALDH1A3-regulated protease genes mediated invasion and metastasis in TNBC

Together, this research identified the ALDH1A3-tPA-plasmin axis as a novel pathway that promotes progressive breast cancer disease.

Copyright Statement

Chapters 2, 3 and 4 have been accepted into:

Bharadwaj A*, McLean ME*, Dahn ML*, Cahill HF, Wasson MCD, Pranap RA, Walker OA, Venkatesh J, Barnes PJ, Bethune G, Knapp G, Helyer L, Giacomantonio CA, Cruickshank BM, Waisman DM, Marcato PP (2023) ALDH1A3 promotes invasion and metastasis in triple-negative breast cancer by regulating the plasminogen activation pathway, *Molecular Oncology*. DOI: 10.1002/1878-0261.13528

Contribution Statement

Alongside other co-first authors, I conducted experiments to understand the role of ALDH1A3 on breast cancer invasion and metastasis through plasminogen activation. I maintained cell lines to complete in vitro and in vivo experiments, performed tissue staining on patient tumours, and aided in manuscript preparation.

Author Contributions: AGB, **MEM**, MLD, MCDW, PM designed the study and performed the experiments, performed data analysis, and data interpretation and wrote the manuscript. HFC, RPA, OLW, BMC, WF, JV and LKH performed the experiments and interpreted the data. PJB, GB, GK, BMC, and CAG provided the materials and reagents for the study and reviewed and edited the manuscript. PM conceptualized and supervised the study and acquired the funding. DMW acquired the funding and supervised the study. All authors edited and revised the manuscript and were involved in the final approval of the manuscript.

Chapter 2 Methods and Materials

2.1 Cell culture and reagents

Cancer cell lines were obtained from ATCC. MDA-MB-231 (RRID: CVCL_0062), MDA-MB-468 (RRID: CVCL_0419), and HEK293T (RRID: CVCL_0063) cells were grown in Dulbecco's Modified Eagle Medium (DMEM; ThermoFisher) supplemented with 10% Fetal Bovine Serum (FBS; ThermoFisher) and antibiotic antimycotic (AA; ThermoFisher). MDA-MB-436 (RRID: CVCL_0623) cells were grown in Leibovitz's Medium (L-15; ThermoFisher) supplemented with 10% FBS, AA, 10μg/mL human insulin (Millipore Sigma), and 16μg/mL L-glutathione (ThermoFisher). Cells were cultured in a humidified 37^{o}C incubator with 5% CO2, except for MDA-MB-436 cells which were cultured without the addition of CO2. The cell lines have been authenticated in the past three years by isolation of genomic DNA and performance of short tandem repeat profiling (STR) technology by Applied Biological Materials Inc. (abm). Abm follows the International Cell Line Authentication Committee (ICLAC) standard ASN-002 in performing the STR analysis. We regularly perform assessments for mycoplasma contamination using the MycoAlert® Mycoplasma Detection Kit (Lonza) and confirm that all experiments were conducted with mycoplasma-free cells.

Cell experiments including ATRA treatments (100nM, Millipore Sigma) were conducted for 24h. For experiments with serum-free conditioned media (SF-CM), MDA-MB-231 cells were cultured using DMEM, without phenol red (21-063-029; ThermoFisher), and sodium pyruvate (ThermoFisher) while MDA-MB-436 cells were cultured in Leibovitz's L-15 Medium, with no phenol red (21083027; ThermoFisher). For assays with plasminogen-depleted media, plasminogen was depleted from FBS by passing the FBS through a lysine sepharose column, which allows the

plasminogen to bind to the column. The flow-through from the lysine sepharose column was collected and filter sterilized using 0.2μm filters (ThermoFisher).

ALDH1A3-over expression for MDA-MB-231 and knockdown of ALDH1A3 in MDA-MB-468 cells was generated as described previously[60,69] and validated by western blotting again here. We also generated shRNA knockdowns in MDA-MB-436 cells using the retroviral vector pSMP (Open Biosystems, Huntsville, AL) with either the shRNAmir scramble sequence or shRNAmir sequences specific to ALDH1A3 (**Table 1**) following standard procedures. The retroviral supernatants were applied to cultured MDA-MB-436 cells. Alternatively, lentiviral short hairpin RNA (shRNA) knockdown clones of *PLAT* were generated using the pGipZ vector (Dharmacon) packaged in HEK293T cells following standard protocols and listed in **Table 1**. Clones were selected by adding 1.5 μg/mL puromycin and subsequently maintained in 0.25 μg/mL puromycin media. Transient knockdown of PLAT was achieved by applying siRNA sequences (Integrated DNA Technologies) with lipofectamine 2000 (ThermoFisher) to cells as per the manufacturer's protocol. The siRNA sequences are listed in (**Table 1)**.

Table 1. shRNA and siRNA sequences and clones

Gene	shRNA	Sequence
ALDH1A3	shRNA1	TGCTGTTGACAGTGAGCGCGCATAGCAAATCCTAGGATAA
	shRNA2	TAGTGAAGCCACAGATGTATTATCCTAGGATTTGCTATGCT

Gene	shRNA	shRNA Used
PLAT	shRNA1	V3LHS_399215
	shRNA2	V2LHS_11084

Gene	siRNA	siRNA Used
PLAT	siRNA1	AAGUGUCAUCAUCGAAUU
	siRNA2	UUCUGUUAAGUAAAUGUU

2.2 Reverse-transcriptase quantitative PCR

For gene expression analysis by reverse-transcriptase quantitative PCR (RT-qPCR) cells were collected in Trizol (ThermoFisher) and RNA was purified using a PureLink RNA kit (ThermoFisher) following the manufacturer's instructions. Equal amounts of purified RNA were then reverse-transcribed to cDNA using iScript (Bio-Rad) as per the manufacturer's instructions. Diluted cDNA was used in RT-qPCR reactions with gene-specific primers (**Table 2**) and SsoAdvanced Universal SYBR Supermix (Bio-Rad) as per manufacturer's instructions with a CFX96 or CFX384 Touch Real-Time PCR Detection System (Bio-Rad). Standard curves were generated for each primer set and primer efficiencies were incorporated into the CFX Manager software (Bio-Rad). Relative expression of genes in cells was quantified using the ΔΔct method of the CFX Manager Software (Bio-Rad), where gene-of-interest quantification was normalized to at least two reference genes (**Table 2**) and then made relative control cells mRNA levels.

Table 2. Gene-specific primers used in RT-qPCR

Target Gene	Forward primer sequence	Reverse primer sequence
B2M	AGGCTATCCAGCGTACTCCA	CGGATGGATGAAACCCAGACA
ARF1	GTGTTCGCCAACAAGCAGG	CAGTTCCTGTGGCGTAGTGA
PUM1	GGCGTTAGCATGGTGGAGTA	CATCCCTTGGGCCAAATCCT
ALDH1A3	TCTCGACAAAGCCCTGAAGT	TATTCGGCCAAAGCGTATTC
PLAT	TGTGTGGAGCAGTCTTCGTT	TCGCTGCAACCTTGGTAAGA
PLAU	GTCACCTACGTGTGTGGAGG	AGTTAAGCCTTGAGCGACCC
SERPINB2	GCAGTTACCCCCATGACTCC	GTGCCTGCAAAATCGCATCA
GAPDH (human)	CAAGGCTGAGAACGGGAAG	GCGAGACCCCACTAACATCA
GAPDH (mouse)	CGCCCCACTTGATTTTGGAG	GGCGGAGATGATGACCCTTT

2.3 Western blotting

Equal concentration protein from cell lysates and conditioned media were separated on 12% SDS-PAGE gels. The proteins were transferred to nitrocellulose or PVDF membranes and blocked with 5% skim milk. The membranes were probed using anti-human ALDH1A3 (OTI4E3, OriGene Technologies), tPA (ab227069, Abcam), uPA (ab24121 Abcam), and PAI-2 (ab47742, Abcam) antibodies. Anti-rabbit HRP-IgG (7074S, Cell Signaling Technology) secondary antibody was used for tPA, uPA, and PAI-2 while anti-mouse HRP-IgG (7076S Cell Signaling Technology) secondary antibody was used for ALDH1A3. Immuno-reactive proteins were detected by chemiluminescence (using Clarity ECL blotting substrate (Bio-Rad)) and visualized with images captured with a ChemiDoc Imager (Bio-Rad). Total protein was used as a loading control.

2.4 Immunofluorescence analysis

Patient tumour core biopsy tissues taken post-surgery from patients who were diagnosed with breast cancer at the Queen Elizabeth II Health Sciences Centre (QEII HSC) in Halifax, Nova Scotia, Canada were analyzed for immunofluorescence staining. Tissues were formalin-fixed and paraffin-embedded. Staff pathologists at the QEII HSC conducted a standard pathological assessment of patient tumours (**Table 3**). 5 μm sections cut from paraffin-embedded blocks were deparaffinized for staining. Post antigen retrieval, and blocking, slides were stained with the above-described antibodies. Secondary IgG antibodies specific to the species for dual labelling were conjugated to either goat anti-rabbit Alexa 488 (A32731 ThermoFisher) or goat anti-mouse Alexa 555 (A32727 ThermoFisher). Nuclei were stained with DAPI (D1306 ThermoFisher). Stained slides were mounted (P36982 ThermoFisher) and images were captured with a Zeiss LSM 880 with an AiryScan laser scanning confocal microscope.

To quantify the number of positive tumour cells in each sample, multiple sections were stained to ensure that representative areas of the entire tissue were assessed. Between three to five random images were captured of each section. A colocalization image creator and colocalization object counter ImageJ plugins were used to semi-automatically count positively stained cells to estimate the percentages of positive tumour cells. This information was then used to calculate the average percentage of ALDH1A3+, tPA+, uPA+, PAI-2+, ALDH1A3+/tPA+, ALDH1A3+/uPA+, and ALDH1A3+/PAI-2- cells within tumour samples.

Table 3. Summary of Patient Tumour Pathology and Clinical Data

Patient ID	Type	Subtype	Staging	Cancer Stage	Tumor Grade	Lymph node Involvement	Progression Free?	Study
P1	IDC	ER+/PR+	T2N1M0	IIB	2	yes	yes	1,2,3
P2	IDC	ER+/PR+/HER2+	T1N1M0	IIA	2	yes	yes	1,2,3
P3	IDC	TNBC	T1N3M0	IIIC	3	yes	yes	1,2,3
P4	IDC	TNBC	T4N1M0	IIIB	3	yes	yes	1,2,3
P5	ILC	ER+/PR+/HER2+	T3N3M0	IIIB	3	yes	no	1,2,3
P6	IDC	ER+/PR+/HER2+	T2N3M0	IIIC	3	yes	yes	1,2,3
P7	IDC	ER+/PR+	T1N0M0	I	2	no	no	1,2,3
P8	IDC	TNBC	T1N0M0	I	3	no	yes	1,2,3
P9	IDC	ER+/PR+/HER2+	T4N3M0	IIIC	3	yes	no	1,2,3
P10	IDC	ER+/PR+	T2N0M0	IIA	1	no	yes	1,2,3
P11	IDC	ER+/PR+/HER2+	T2N0M0	IIA	3	no	no	1,2,3
P12	IDC	ER+/PR+	T2N0M0	IIA	3	no	no	1,2,3
P13	IDC	ER+/PR+	T2N0	IIA	3	no	no	1,2,3
P14	IDC	TNBC	T2N1M0	IIB	3	yes	no	1,2,3
P15	IDC	ER+/PR+	T2N1M0	IIB	2	yes	no	1,2,3
P16	IDC	ER+/PR+/HER2+	T1N1M0	IIA	3	yes	no	1,2
P17	ILC	ER+/PR+	T2N1M0	IIB	2	yes	yes	1,3
P18	IDC	ER+/PR+	T2N1M0	IIB	3	yes	no	1,2,3
P19	IDC	HER2+	T2N0M0	IIA	3	no	yes	1,2,3
P20	IDC	ER+/PR+	T1N2M0	IIIA	3	yes	yes	1,2,3
P21	IDC and ILC	ER+/PR+	T2N0MO	IIA	2	no	yes	1,2
P22	IDC	ER+	T1N0M0	I	1	no	no	1,2,3
P23	IDC	ER+/PR+	T2N0M0	IIA	2	no	yes	1,2,3
P24	IDC	ND	T1micN0	I	3	no	yes	1,2,3
P25	ILC and IDC	ER+/PR+	T2N0	IIA	2	no	yes	1,2,3
P26	IDC	ER+/HER2	T1cN1M0	IIA	3	yes	yes	1,2,3
P27	IDC	ER+/PR+	T2N1a	IV	2	yes	yes	1,2,3
P28	IDC	ER+/PR+	T2N0M0	IIA	3	no	no	1,2,3
P29	IDC	ER+/PR+/HER2+	T1cN0M0	I	2	no	yes	1,2,3
P30	IDC	ER+/PR+/HER2+	T1cN0M0	I	2	no	yes	1,3
P31	IDC	ER+/PR+	T2N0M0	IIA	2	no	no	1,2,3
P32	IDC	TNBC	T2N1M0	IIB	3	yes	yes	1,2,3
P33	ILC	ER+/PR+	T2N1	IIB	2	yes	yes	1,2,3
P34	IDC	ER+/PR+	T2N2aM0	IIIA	1	yes	yes	1,2,3

Patient ID	Type	Subtype	Staging	Cancer Stage	Tumor Grade	Lymph node Involvement	Progression Free?	Study
P35	IDC	ER+/PR+	T2N2aM0	IIIA	1	yes	yes	1
P36	IDC	ER+/PR+	T3	IIIB	2	yes	yes	1,2,3
P37	IDC	TNBC	T2,N0	IIA	3	no	yes	1,2,3
P38	IDC	TNBC	T2N2	IIIa	3	yes	yes	1,2,3
P39	IDC	ER+/PR+	T2N0	IIA	2	no	no	1,2,3
P40	IDC	TNBC	T1N0	I	3	no	yes	1,2,3
P41	IDC	ER+	T2N2	IIIA	2	yes	yes	1,2,3
P42	ILC	ER+/PR+	T1b	I	2	no	yes	1,2,3
P43	IDC	ER+/PR+/HER2+	T2N1	IIB	3	yes	no	1,2,3
P44	IDC	ER+/PR+	T1N0	I	2	no	yes	1,2,3
P45	ILC	ER+/PR+	T1	I	3	no	no	1,2
P46	IDC	TNBC	T2N0	IIA	3	no	no	1,2,3
P47	IDC	ER+/PR+/HER2+	T1N0	I	3	no	yes	1,2,3
P48	IDC	TNBC	T1N0	I	3	no	no	1,2,3
P49	DCIS	TNBC	T4 N1 M0	IIIB	3	Yes	yes	1,2,3
P50	DCIS	TNBC	Tis N0 N0	I	2	No	yes	1,2,3
P51	DCIS and IDC	TNBC	T1 N0 M0	I	3	No	yes	1,2,3
P52	IDC	TNBC	T4 N0 M0	IIIB	3	No	yes	1,2,3
P53	DCIS and IDC	TNBC	T1 N1 M0	IIA	3	Yes	yes	1,2,3
P54	DCIS and IDC	TNBC	T1 N0 M0	I	2	No	no	1,2,3
P55	DCIS and IDC	TNBC	T2 N0 M0	IIA	3	Yes	yes	1,2,3
P56	DCIS and IDC	TNBC	T2 N1 M0	IIB	3	Yes	yes	1,2,3
P57	DCIS and IDC	TNBC	T1 N0 M0	I	3	No	yes	1,2,3
P58	IDC	TNBC	T2 N1 M0	IIB	3	yes	no	1,2,3
P59	IDC	TNBC	T3 N2 M0	IIIA	3	yes	no	1,2,3
P60	IDC	TNBC	T1 N1 M0	IIA	3	yes	yes	1,2,3
P61	IDC	TNBC	T1 N0 M0	IA	3	yes	yes	1,2,3
P62	IDC	TNBC	T2 N1 M0	IIB	3	yes	no	1,2,3
P63	IDC	TNBC	T1 N2 M0	IIIA	3	yes	no	1,2,3
P64	IDC	TNBC	T2 N0 M0	IIA	3	no	yes	1,2,3
P65	IDC	TNBC	T2 N3 M0	IIIC	3	yes	yes	1,2,3

Patient ID	Type	Subtype	Staging	Cancer Stage	Tumor Grade	Lymph node Involvement	Progression Free?	Study
P66	IDC	TNBC	T1 N1 M0	IIA	3	yes	yes	1,2,3
P67	IDC	TNBC	T2 N0 M0	IIA	3	no	no	1,2,3
P68	IDC	TNBC	T2 N0 M0	IIA	3	no	yes	1,2,3
P69	IDC	TNBC	T1 N0 M0	IA	3	no	yes	1,2,3
P70	IDC	TNBC	T1 N0 M0	IA	3	no	no	1,2,3
P71	IDC	TNBC	T1 N0 M0	IA	3	no	yes	1,2,3
P72	IDC	TNBC	T1 N1 M0	IIA	3	yes	yes	1,2,3
P73	IDC	TNBC	T1 N0 N0	IA	3	no	no	1,2,3
P74	IDC	ER+/PR+	T2N0M0	IIA	1	no	no	2,3
P75	IDC	ER+/PR+	T2N0M0	IIA	3	no	no	3
P76	IDC	ER+/PR+	T2N1M0	IIB	2	yes	yes	3
P77	IDC	ER+/PR+	T2N1	IIB	3	yes	yes	2,3
P78	IDC	TNBC	T2N0M0	IIA	3	yes	yes	2

Abbreviations and Definitions

IDC = Invasive ductal carcinoma
ILD = Invasive lobular carcinoma
DCIS = Ductal carcinoma in situ

T1: tumour of 2cm or less
T2: tumour between 2cm and 5cm
T3: tumour more than 5cm
T4: tumour of any size with extension to chest wall or skin

N0: no lymph node involvement
N1: 1-3 lymph nodes involved
N2: 4-9 lymph nodes involved
N3: 10 or more lymph nodes involved

M0 = distal metastasis not present
M1 = distal metastasis present

Grade: Modified Bloom Richardson grading scheme based on three morphological features; degree of tumour tubular formation, tumour mitotic activity, nuclear pleomorphism of tumour cells. Higher grade is associated with worse prognosis.

ER: Estrogen receptor
PR: Progesterone receptor
HER-2/neu: Human epidermal growth factor receptor 2
ND: Not determined

Study 1: ALDH1A3 and tPA stained

Study 2: ALDH1A3 and uPA stained
Study 3: ALDH1A3 and PAI-2 stained

2.5 Cell surface plasminogen activation assay

Cells were seeded at a density of 30,000 cells/well in 96-well plates (Corning) overnight and washed three times with incubation buffer (Hanks balanced salt solution containing 3 mM $CaCl_2$ and 1 mM $MgCl_2$; ThermoFisher). For experiments with siRNA, the cells were transfected with the siRNA before the commencement of the experiment. Cells were then incubated with 0.5 μM Glu-plasminogen (Molecular Innovations, Michigan, USA), for 15-20 minutes at 37^0C before the addition of 500 μM plasmin chromogenic substrate (S2251, Chromogenix, Diapharma Group). Plasmin activity was measured spectrophotometrically (405 nm) taking readings every 2 minutes for 2 hours. Time course data were analyzed according to the equation describing the p-nitroanilide (p-NA) production rate $A405\ nm = B + Kt2$, where K is the rate constant for the acceleration of *p*-NA generation and B is the *y*-intercept. Under our experimental conditions, K is proportional to the initial rate of plasmin formation from plasminogen.

2.6 tPA and uPA activation assays

Cells were seeded at 2-3x10^6 cells per plate and serum starved after 24 hours of incubation. For experiments with siRNA, the cells were transfected with the siRNA for 48h before measuring cell surface plasminogen activation and 72h for measuring tPA activity in CM. Specifically for tPA activity in CM, siRNA transfected cells were conditioned in serum-free media after 24h post-transfection for 48 hours, before the determination of the activities. The serum-free conditioned media (SF-CM) was harvested after 48-72 hours of conditioning and then centrifuged at 2000 g for 15-20 minutes to remove cell debris. The SF-CM was concentrated using Amicon centrifugation filter devices (ThermoFisher) with a 30 kD molecular weight cut-off. The protein concentration in the SF-CM was determined using a BCA assay and equal protein amounts (50 μg) were used for tPA and uPA activity assays. The tPA activity was determined using 0.5mM

tPA substrate S2288 (Diapharma, OH, USA), and uPA activity was determined using 0.5mM of uPA substrate cs-uk-dpg444-25 (Diapharma, OH, USA). Briefly, the SF-CM and respective substrates were mixed and activity was measured spectrophotometrically (405 nm) taking readings every 2 minutes for 2 hours at 37^0C. Time course data were analyzed according to the equation describing the p-nitroanilide (p-NA) production rate $A405\ nm = B + Kt$t, where K is the rate constant for the acceleration of *p*-NA generation and B is the *y*-intercept.

2.7 Transwell invasion assay

2.5×10^4 cells were seeded in the upper well of either a Matrigel-coated invasion chamber (Corning) or an uncoated migration chamber (Corning) with 8 μm pore size in serum-free media, with 10% FBS containing media in the bottom well as a chemoattractant. For experiments with siRNA, the cells were transfected with the siRNA for 24 hours before the commencement of the experiment. For the experiments with plasminogen-stripped FBS, the bottom chamber contained 10% plasminogen-stripped FBS as a chemoattractant +/- 0.25μM plasminogen (Molecular Innovations, Michigan, USA). We added plasminogen to the bottom chamber along with plasminogen-stripped FBS to replicate the "unstripped" regular FBS, which is normally used in transwell invasion assays and has plasminogen among its components. The FBS in the bottom well acts as a chemoattractant, but it also freely diffuses into the top well. Like other FBS components, plasminogen in the bottom well would diffuse into the upper chamber and be accessible to cells to activate into plasmin. After 24 hours, migrated or invaded cells that had crossed the chamber membrane were fixed in methanol and stained with 0.05% crystal violet. Transversed cells were counted in four to five fields of view per chamber at 20X using a Motic AE31E light microscope. Motic Motican72 technology. The percent invasion was determined via the following equation:

$$\%Invasion = \frac{meannumberofcellsinvadedthroughMatrigel - coatedtranswell}{meannumberofcellsmigratedthroughuncoatedtranswell} x100$$

2.8 Orthotopic tumour xenograft experiment

All experiments followed guidelines set by the Canadian Council on Animal Care and were performed according to a protocol approved by the Dalhousie University Committee on Laboratory Animals (protocol 21-011). Seven-week-old NOD/SCID female mice were orthotopically injected in the mammary fat pad four with 2×10^6 cells of MDA-MB-231 with or without PLAT (tPA) knockdown along with a 1:1 ratio of high concentration Matrigel (Corning, VWR). Primary tumour growth was quantified (length × length × height/2). At termination, the lungs, the axillary and inguinal lymph nodes, and tumours were harvested for analysis. The lungs (minus the left lung lobe that was stored in RNAlater reagent for later analysis by RT-qPCR) and nodes were fixed, paraffin-embedded and sectioned (5μm) for metastasis visualization by hematoxylin and eosin (H&E) or stained by immunofluorescence with a pan-cytokeratin antibody (Dako, M3515) and secondary anti-mouse antibody described above. H&E-stained sections were imaged using an Aperio Scanning system (Leica Biosystems, Concord, Ontario) at 2×magnification and a further 10X zoom magnification of cropped images was done as indicated in legends as indicated.

2.9 Quantification disseminated MDA-MB-231 cells in the lungs of mice by human-specific GAPDH RT-QPCR

To quantify the number of MDA-MB-231 cells in the left lung lobe from the above-described experiment, we used our previously published method that can accurately quantify between 100 – 1 000 000 disseminated human cells in mouse lungs[132], Briefly, the RNA was

extracted from the lung lobes and RT-qPCR performed as described above. In the RT-qPCR assay, we used our previously validated human-specific and mouse GAPDH primers[132] (**Table 2**). The number of MDA-MB-231 cells detected in the lung lobes was calculated based on a standard curve generated from RNA extracted from naïve lung lobes that had been spiked with increasing numbers of MDA-MB-231 cells (ranging from 10 to 1 000 000 cells).

2.10 Transcriptome, 450K methylation, and patient dataset analysis

Microarray gene expression data for MDA-MB-231 control and overexpressing ALDH1A3 (n=3; GSE103426) was analyzed. Breast Cancer (METABRIC, TNBC, hormone receptor-positive, or HER2+ patient tumours, or normal adjacent tissues within the dataset) and Breast Invasive Carcinoma (TCGA, Cell 2015; TNBC, hormone receptor-positive, or HER2+ patient tumours within the dataset) clinical data and RNA sequencing (RNA-seq) log2 V2 RSEM and gene array expression data were accessed via cBioportal[133,134]. CpG methylation of PLAT and PLAU in MDA-MB-231 and MDA-MB-436 cell lines was determined by analyzing 450K methylation data (GSE78875). The corresponding methylation of specific CpG sites in PLAT and PLAU was accessed from the 450K methylation data from the TCGA Firehose cohort obtained from the Broad Institute GDAC portal.

2.11 Statistical Analyses

All statistical analyses were calculated in GraphPad Prism 9. T-tests were performed when two experimental conditions were compared. In cases when multiple conditions were tested, one-way ANOVA analyses were performed followed by multiple comparisons analysis. Pearson and Spearman correlation coefficient analyses were conducted on gene expression correlations of

patient tumour data. A log-rank test was conducted on Kaplan-Meier overall and progression-free survival curve analyses. P values are represented as follows: * = <0.05, ** = <0.01, *** = <0.001, **** = <0.0001. Statistical tests and significance are indicated in all figure captions.

Chapter 3 Results

3.1 ALDH1A3 is co-expressed with factors in the plasminogen activation pathway in TNBC

We have shown that ALDH1A3 mediates invasion and metastasis in TNBC, which is at least in part attributable to gene expression changes induced by ALDH1A3[69]. Therefore, to investigate potential mechanisms for ALDH1A3-mediated invasion, we assessed the TCGA RNAseq and METABRIC gene array data for gene co-expression with ALDH1A3 in TNBC tumours. In the graphs, genes with high positive Spearman and Pearson correlations are positively co-expressed with ALDH1A3, while genes with low negative Spearman and Pearson correlations are negatively co-expressed with ALDH1A3 (**Fig. 1A**). We focused our analysis specifically on the 86 genes that are proteases or regulators of proteases known to mediate the degradation of the extracellular matrix in cancer progression (**Fig. 1A**). In both patient data sets, we noted significant positive co-expression between ALDH1A3 and transmembrane serine protease 2 (TMPRSS2), MMP2, 3 and 11, and PLAT and PLAU that encode the plasminogen activators, tPA and uPA, respectively.

Although these co-expression analyses in patient tumour data suggest a potential connection between ALDH1A3 and these proteases and protease regulators, it does not necessarily mean direct regulation of the genes by ALDH1A3. Therefore, we assessed the same 86 genes in our gene array data of TNBC MDA-MB-231 cells, with or without ALDH1A3 overexpression. Among the genes, the two most prominent ALDH1A3-regulated genes in MDA-MB-231 cells are PLAT (encodes tPA), and SERPBINB2 (encodes PAI-2, an inhibitor of tPA and uPA) (**Fig. 1B**). ALDH1A3 also upregulated MMP1 and MMP8; however, these were not highly co-expressed with ALDH1A3 in the patient tumour data (**Fig. 1A**). We also noted that ALDH1A3 upregulated TIMP metallopeptidase inhibitor 3 (TIMP3) in MDA-MB-231 cells (**Fig. 1B**), and

TIMP3 was highly co-expressed with ALDH1A3 in the TCGA Cell 2015 patient tumour dataset (**Fig. 1A**). TIMP3 is a well-known inhibitor of the MMPs and a disintegrin and metalloproteinases (ADAMs), and ADAM with thrombospondin motifs (ADAMTSs) proteins[135,136]. The upregulation of TIMP3 by ALDH1A3 suggests the metalloproteases could be inhibited in high-ALDH1A3 expressing cells making metalloprotease-mediated invasion by ALDH1A3 in the cells less likely. Together, the patient tumour and cell line expression data most consistently implicated the plasminogen activation pathway could be important in ALDH1A3-mediated invasion. We, therefore, confirmed the ALDH1A3-dependent regulation of PLAT, PLAU, and SERPINB2 by RT-qPCR (**Fig. 1C**) and visualized the co-expression correlation of the genes with ALDH1A3 in the patient tumour data (**Fig 1D**). We similarly noted generally similar co-expression of these genes with ALDH1A3 in hormone receptor+ breast cancers (**Fig. 2A)**, normal adjacent tissues (**Fig. 2B**) and TNBC cell lines (**Fig. 2C**). Interestingly, in HER2+ breast cancers, ALDH1A3 expression did not correlate with PLAT expression (**Fig 2D**). The co-expression of PLAT and PLAU in TNBC patients and cell lines with ALDH1A3 is consistent the regulation of the genes by ALDH1A3 in MDA-MB-231 cells. In contrast, SERPINB2 was not negatively co-expressed in all patient tumours and normal adjacent samples as expected. Together the patient tumour and cell line data prompted us to prioritize our investigation on the effects of ALDH1A3 on the plasminogen activation pathway and if this pathway contributes to ALDH1A3-mediated invasion and metastasis in TNBC.

Figure 1

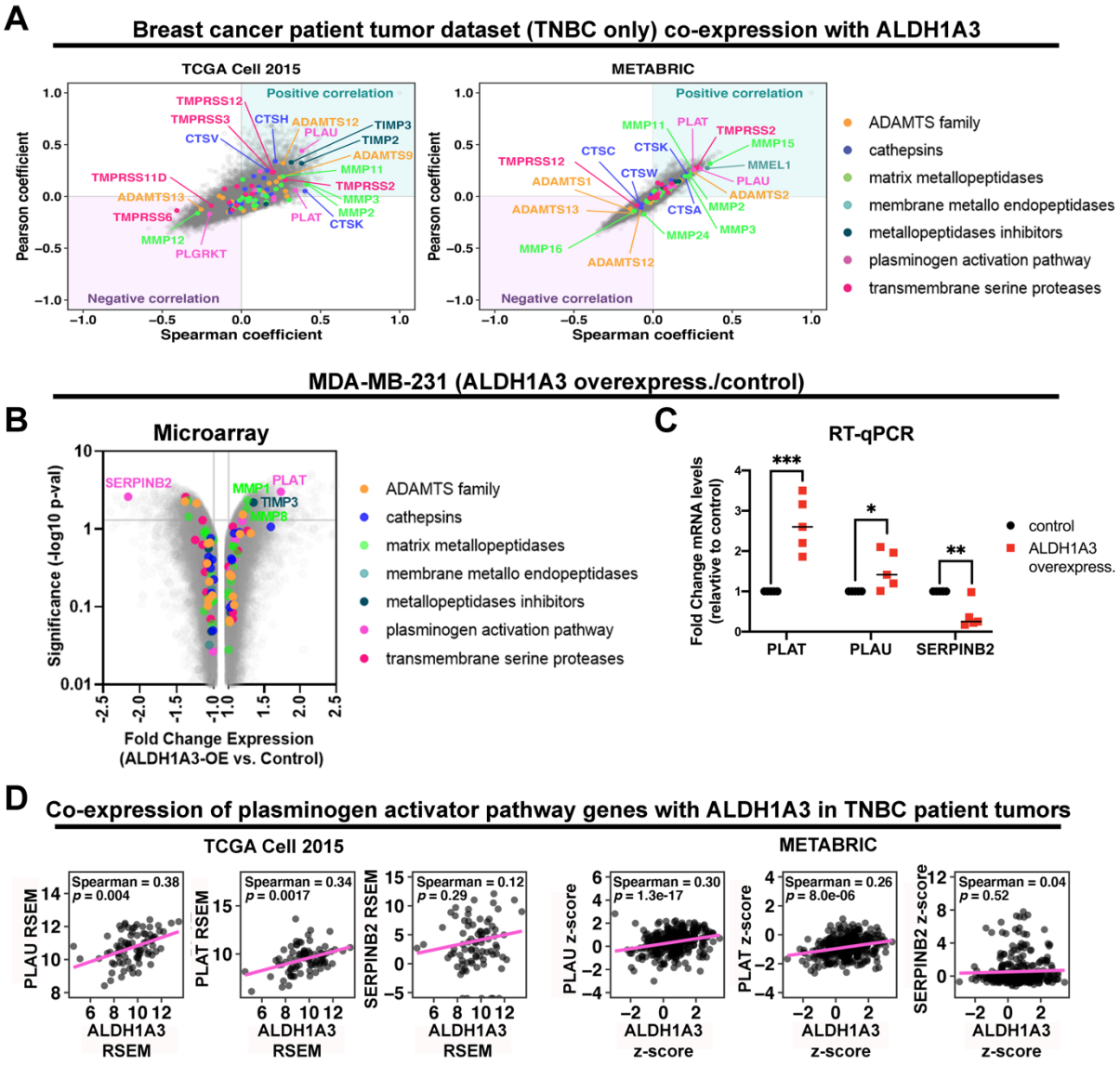

Figure 1. ALDH1A3 co-expressions and regulates genes in the plasminogen activation pathway in TNBC. (A) Pearson and Spearmen coefficients were calculated based on the co-expression of ALDH1A3 and all the genes in the subset of patients identified as TNBC in the METABRIC (n=320); TCGA, Cell 2015 (n=82); RNA-Seq RSEM log2. Proteases or protease regulators are identified (**Table 4**). **(B)** Transcriptome analysis of MDA-MB-231 cells (ALDH1A3 overexpression versus control cells) completed by Affymetrix Human Gene 2.0ST Array (n=3; GSE103426) identified differential expression of protease or protease regulator genes, the grey horizontal line indicates p<0.05. **(C)** RT-qPCR of MDA-MB-231 cells (ALDH1A3 overexpression versus control cells), n =5, significance determined by paired t-test. (**D**) Co-expression analysis of ALDH1A3 versus PLAU, PLAT, and SERPINB2 in TNBC patient samples from TCGA Cell 2015 and METABRIC datasets. Spearman coefficient and adjusted p values are indicated

Figure 2

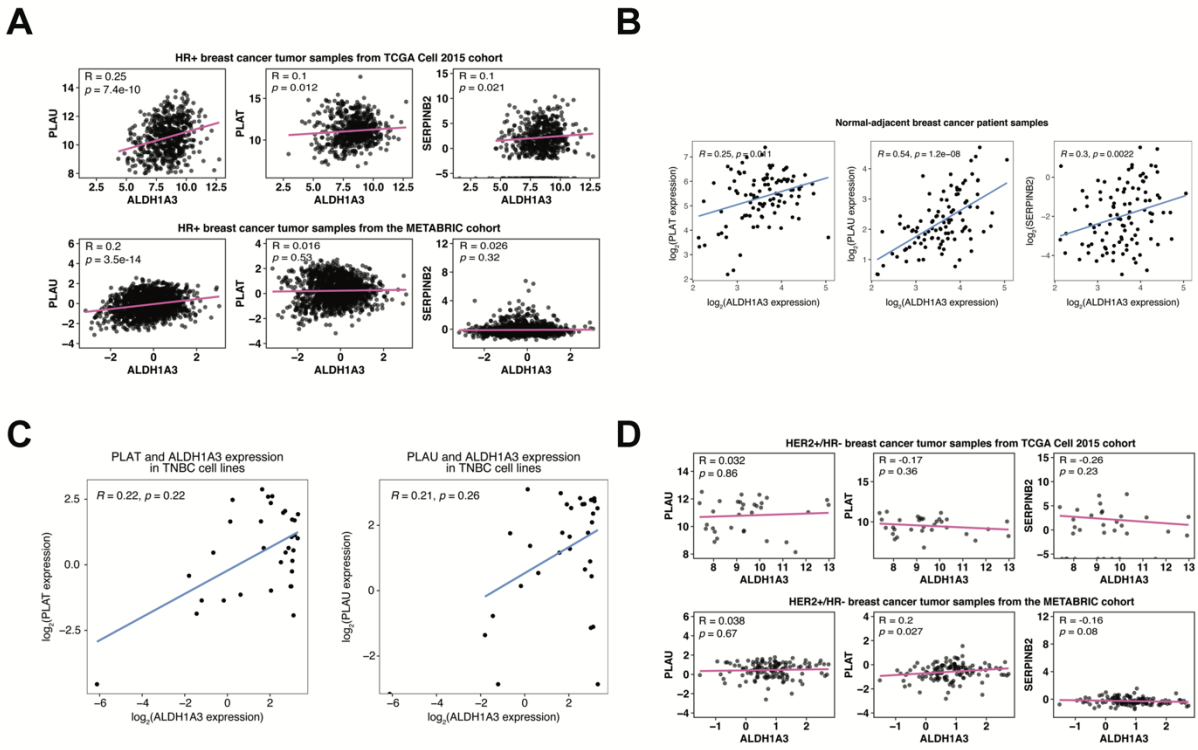

Figure 2. ALDH1A3 correlations with PLAU, PLAT and SERPINB2 in HR+, TNBC and normal adjacent breast cancer samples. **(A)** RNA-sequencing expression from HR+ breast cancer patient tumour samples from the TCGA Cell 2015 cohort (top panel) and METABRIC cohort (bottom panel) were obtained from cBioPortal. HR+ patients were identified and extracted (TCGA: n = 593, METABRIC: n = 1478). **(B)** RNA-sequencing expression for PLAT, PLAU, SERPINB2 and ALDH1A3 in normal-adjacent breast cancer patient samples were obtained from the TCGA Firehose cohort accessed through the Broad Institute GDAC portal. Normal-adjacent samples were identified and extracted based on the TCGA tumour barcode (n = 100). **(C)** RNA-sequencing expression for PLAT, PLAU and ALDH1A3 in triple-negative breast cancer (TNBC) cell lines (n = 33) were obtained from the Cancer Cell Line Encyclopedia (CCLE). The Spearman coefficient (R) and corresponding p-value are shown for each correlation. **(D)** RNA-sequencing expression from HER2+/HR- breast cancer patient tumour samples from the TCGA Cell 2015 cohort (top panel) and METABRIC cohort (bottom panel) were obtained from cBioPortal. HER2+ patients were identified and extracted (TCGA: n = 32, METABRIC: n = 127).

Table 4. Families of Proteases or Regulators of Proteases Genes Implicated in the Remodeling of the Extracellular Matix

ADAMTS family	cathepsins	matrix metallo-peptidases	membrane metallo-endopeptidases	plasminogen activation pathway	Trans-membrane serine proteases	Metallo-peptidases inhibitors
ADAMTS1	CTSA	MMP1	MME	PLG	TMPRSS11A	TIMP1
ADAMTS10	CTSB	MMP10	MMEL1	PLAT	TMPRSS11B	TIMP2
ADAMTS12	CTSC	MMP11		PLAU	TMPRSS11D	TIMP3
ADAMTS13	CTSD	MMP12		PLAUR	TMPRSS11E	TIMP4
ADAMTS14	CTSE	MMP13		PLGRKT	TMPRSS11F	
ADAMTS15	CTSF	MMP14		SERPINB2; SERPINB10	TMPRSS12	
ADAMTS16	CTSG	MMP15		SERPINE1	TMPRSS13	
ADAMTS17	CTSH	MMP16			TMPRSS15	
ADAMTS18	CTSK	MMP17			TMPRSS2	
ADAMTS19	CTSL	MMP19			TMPRSS3	
ADAMTS2	CTSO	MMP2			TMPRSS4	
ADAMTS20	CTSS	MMP2			TMPRSS5	
ADAMTS3	CTSV	MMP20			TMPRSS6	
ADAMTS4	CTSW	MMP21			TMPRSS7	
ADAMTS5	CTSZ	MMP23A; MMP23B			TMPRSS9	
ADAMTS6		MMP23B; MMP23A				
ADAMTS7		MMP24				
ADAMTS8		MMP25				
ADAMTS9		MMP26				
		MMP27				
		MMP28				
		MMP3				
		MMP7				
		MMP8				

ADAMTS family	cathepsins	matrix metallo-peptidases	membrane metallo-endopeptidases	plasminogen activation pathway	Trans-membrane serine proteases	Metallo-peptidases inhibitors
		MMP9				

3.2 ALDH1A3 increases plasmin and ALDH1A3-mediated invasion is plasminogen-dependent in TNBC cells

We first confirmed that plasmin generation is altered by ALDH1A3 in TNBC cell lines by performing a cell surface plasminogen activation assay. Plasminogen is an inactive zymogen that is synthesized and secreted in the systemic circulation by the liver[137]. Plasminogen binds to cell surface receptors where it becomes cleaved by extracellular tPA and/or uPA which generates activation of the plasmin protease. In an *in vitro* plasmin activity assay, washed cell monolayers are treated with plasminogen and the subsequent generation of active plasmin is measured by hydrolysis of the synthetic substrate and the release of the chromophore pNA (chromophore).

For these assays, we again used the TNBC MDA-MB-231 cells, with or without ALDH1A3 overexpression, as well as TNBC MDA-MB-436 and MDA-MB-468 cells, in which we knocked down ALDH1A3 (**Fig. 3A**). We chose this approach because ALDH1A3 is intrinsically low in MDA-MB-231 cells, but higher in MDA-MB-436 and MDA-MB-468 cells. We observed that the plasmin activity was positively correlated with the ALDH1A3 expression levels in these cell lines, with higher activity of plasmin in ALDH1A3 overexpressing MDA-MB-231 cells and lower activity upon reduction in ALDH1A3 expression by knockdown in MDA-MB-436 cells and MDA-MB-468 cells (**Fig. 3B**).

We next assessed the functional relevance of this activity in cancer. Protease activity is essential for the degradation of the extracellular matrix and is required for breast cancer cell invasion. We first confirmed the invasive capacity of the TNBC cell lines and noted that ALDH1A3 overexpression in MDA-MB-231 cells increased invasion and ALDH1A3 knockdown in MDA-MB-436 and MDA-MB-468 knockdown decreased invasion (**Fig. 3C).** We noted that the increase in invasion imparted by ALDH1A3 (**Fig. 3C**) was greater than the plasmin activity induced by ALDH1A3 (**Fig. 3B**). This could be due to several reasons. First, the generation of

active plasmin as measured by hydrolysis of a synthetic substrate and the release of the chromophore pNA is not likely to translate equally into units of invasion as measured by a transwell assay. Invasion mediated by plasmin can also be enhanced by activation of MMPs by plasmin, hence the 1.5-fold difference in plasminogen activity could result in an amplified 3-fold increase in invasion. Repeating the transwell invasion assay with plasminogen-depleted FBS impeded ALDH1A3-dependent invasion, which was restored with the exogenous addition of plasminogen **(Fig. 3D).** Together these findings illustrate that ALDH1A3 regulates plasmin activity in TNBC, and a component of ALDH1A3-dependent invasion is dependent on these ALDH1A3-dependent changes in the invasion of TNBC cells.

Figure 3

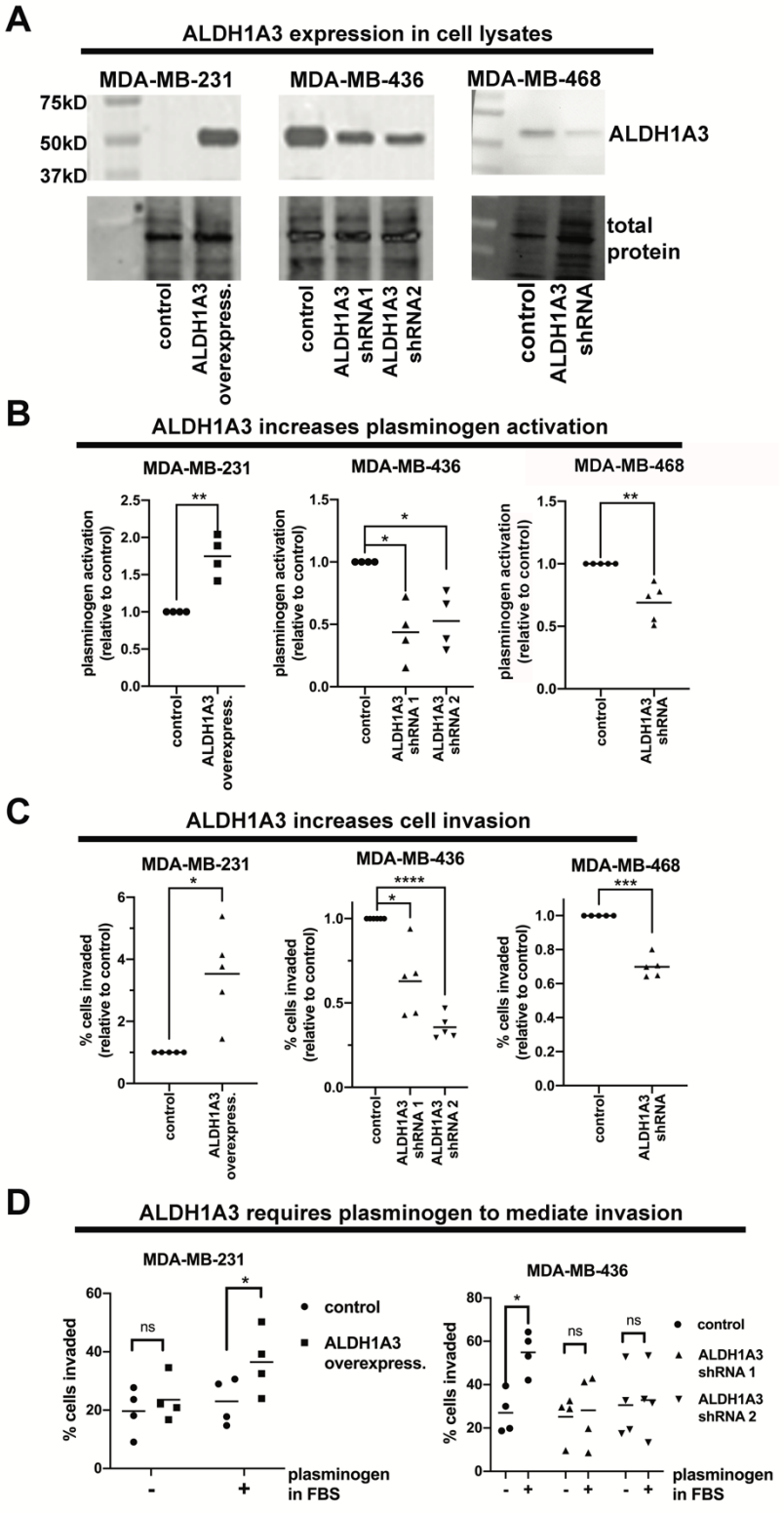

Figure 3. ALDH1A3 increased invasion is dependent on plasminogen activation. (A) Western blots confirmed overexpression of ALDH1A3 in MDA-MB-231 and reduced expression of

ALDH1A3 in MDA-MB-436 and MDA-MB-468 cells. **(B)** The cell surface plasminogen activation assay was performed in MDA-MB-231 cells (vector control versus ALDH1A3 overexpression compared), MDA-MB-436 cells (shRNA scramble control versus shRNA 1 and 2 compared) and MDA-MB-468 cells (shRNA scramble control versus shRNA 2 compared). Values are relative to control cells (n=4 or 5). **(C, D)** Transwell invasion assays were completed with MDA-MB-231 cells (vector control versus ALDH1A3 overexpression compared), MDA-MB-436 cells (shRNA scramble control versus shRNA 1 and 2 compared) and MDA-MB-468 cells (shRNA scramble control versus shRNA 2 compared) with FBS as a chemoattractant (**C**) or with plasminogen-stripped FBS and plasminogen added back as indicated (**D**) for MDA-MB-231 and MDA-MB-436 cells. (**B, C, D**) Significance was determined by t-test for experiments with MDA-MB-231 and MDA-MB-468 cells and by one-way ANOVA followed by multiple comparison tests for experiments with MDA-MB-436 cells. Significant p values are indicated as follows: * = <0.05, ** = <0.01, *** = <0.001.

3.3 ALDH1A3 increases extracellular tPA and/or uPA proteins and activity in TNBC cells

We next investigated the molecular mechanism for the regulation of plasmin activity by ALDH1A3 in TNBC cells (**Fig. 3B**). Using gene expression analysis of TNBC patient tumours and MDA-MB-231 cells, we found evidence of increased tPA and uPA, and decreased PAI-2 (**Fig. 1**). PAI-2 inactivates tPA and uPA, leading to their degradation[138]; so decreased PAI-2 expression could also contribute to increased plasmin activity.

We assessed the secreted tPA levels in MDA-MB-231, MDA-MB-436, and MDA-MB-468 cells by performing western blots and tPA activity assays of the concentrated conditioned media from the cells (**Fig. 4A).** In MDA-MB-231 and MDA-MB-468 cells we detected secreted tPA, which was increased upon ALDH1A3 overexpression in MDA-MB-231 cells and decreased upon ALDH1A3 knockdown in MDA-MB-468 cells (**Fig. 4A**). Overexpression of ALDH1A3 in MDA-MB-231 also significantly increased the tPA activity and decreased tPA activity in MDA-MB-468 cells (**Fig. 4A**). In contrast, we failed to detect secreted tPA by MDA-MB-436 cells.

We next assessed secreted uPA levels and activity in MDA-MB-231, MDA-MB-436 and MDA-MB-468 cells (**Fig. 4B**). ALDH1A3 increased the expression of secreted uPA in MDA-MB-231 cells. In MDA-MB-436 and MDA-MB-468 cells we detected secreted uPA, which was decreased by ALDH1A3 knockdown. To assess for secreted uPA activity, we performed uPA activity assays in the conditioned media from the cells and consistent with the western blots, uPA activity was increased by ALDH1A3 overexpression in MDA-MB-231 cells and decreased by ALDH1A3 reduction in the MDA-MB-436 and MDA-MB-468 cells with ALDH1A3 knockdown **(Fig. 4B).**

We followed up on the observed SERPINB2 gene expression changes (**Fig. 1)** by assessing the levels of PAI-2 in MDA-MB-231 and MDA-MB-436 cells. PAI-2 is an intracellular protein

and exerts its inhibitory activity intracellularly[139]. In MDA-MB-231 cells, PAI-2 was decreased by ALDH1A3 overexpression; however, in MDA-MB-436 and MDA-MB-468 cells PAI-2 was undetectable (**Fig. 4C**). In MDA-MB-231 cells, the decreased PAI-2 could contribute to the increased tPA, uPA, and plasmin activity induced by ALDH1A3; however, given its absence in MDA-MB-436 and MDA-MB-468 cells, its role in ALDH1A3-mediated plasmin activity in the breast cancer cells may be less important. Consistent with this finding in the MDA-MB-436 cells, the results from the patient tumour data also suggested that there was no correlation between ALDH1A3 and SERPINB2 expression (**Fig. 1D**). Together these data suggest that the increased plasmin activity by ALDH1A3 in TNBC could be due to both to increased secreted tPA and uPA, with some cell line-specific effects in the dominance of one plasminogen activator over the other.

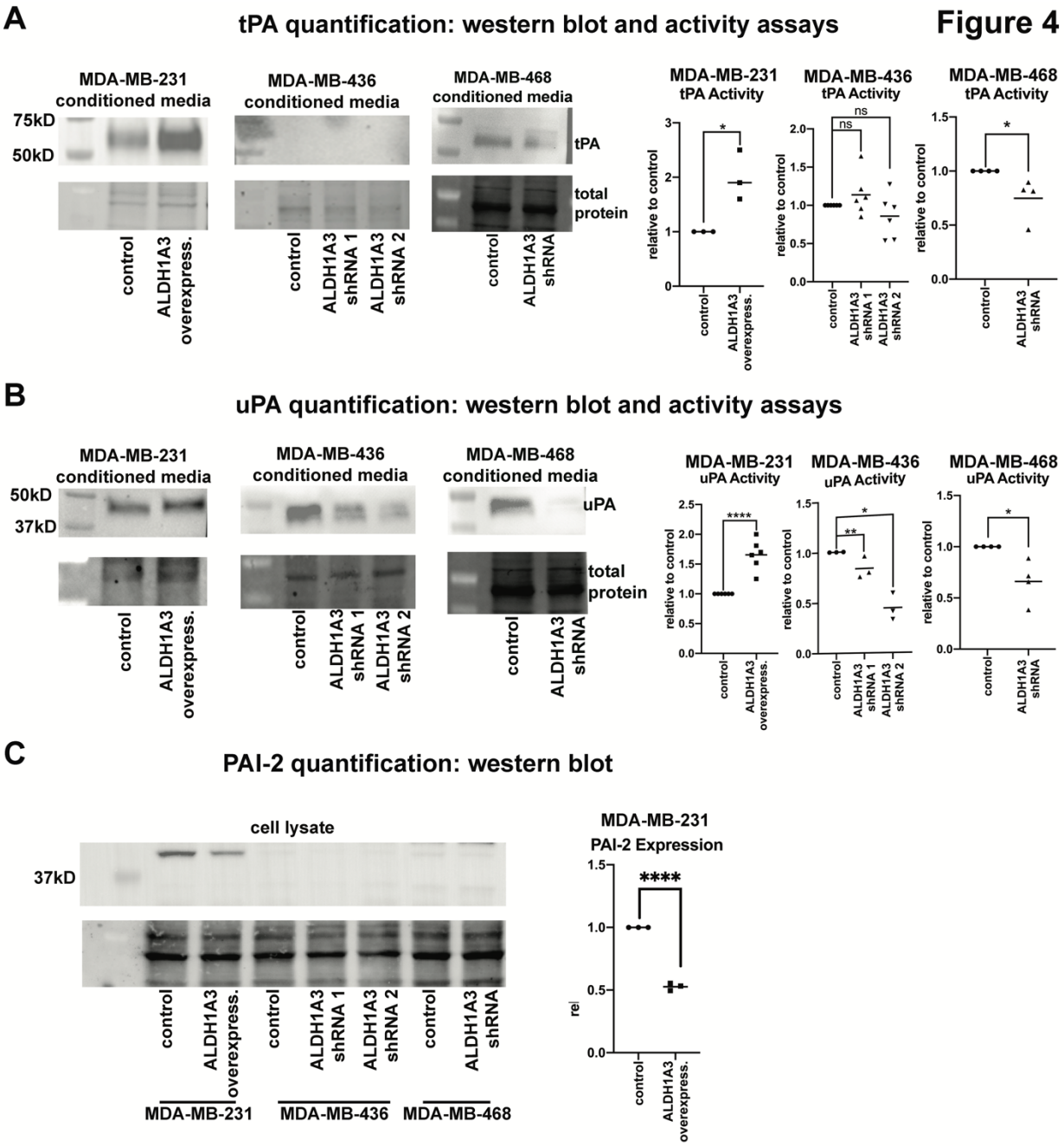

Figure 4. ALDH1A3 regulation of tPA, uPA, and PAI-2 proteins and tPA and uPA activity in TNBC cells. (A, B) Secreted tPA (**A**) and uPA (**B**) is detected in the conditioned media of MDA-MB-231 (vector control versus ALDH1A3 overexpression compared), MDA-MB-436 cells (shRNA scramble control versus shRNA 1 and 2 compared) and MDA-MB-468 cells (shRNA scramble control versus shRNA 2 compared) by western blots and activity assays (individual n are shown in the assays) . tPA was not detected in conditioned media from MDA-MB-436 cells. **(C)** PAI-2 is detected in the cell lysates of MDA-MB-231 (vector control versus ALDH1A3 overexpression compared, n=3) but not detected in the cell lysates of MDA-MB-436 or MDA-MB-468 cells. (**A-C**) Significance was determined by t-test for experiments with MDA-

MB-231 and MDA-MB-468 cells and by one-way ANOVA followed by multiple comparison tests for experiments with MDA-MB-436. Significant p values are indicated as follows: * = <0.05, ** = <0.01, *** = <0.001, **** = <0.0001.

3.4 DNA methylation and ATRA affect PLAT expression

Having demonstrated that ALDH1A3 increases plasmin activity in TNBC cells by mediating alterations in gene and protein expression of key players of the plasminogen activation pathway in the cells, we next evaluated the mechanistic basis for the activation of these genes. We were also interested in exploring potential mechanistic reasons for the lack of detectable tPA/PLAT in MDA-MB-436 cells (**Fig. 4A**). In our previous work on the mechanisms of ALDH1A3 in breast cancer, we found that DNA methylation of ALDH1A3/ATRA inducible genes plays a major role on in if a gene can be induced by ALDH1A3/ATRA. Genes with hypermethylated transcription start sites (TSS) and promoter regions are poorly inducible by ALDH1A3[69,140,141]. We therefore analyzed the CpG methylation of PLAT (encodes tPA) and PLAU (encodes uPA) by analysing the 450K CpG methylation data of the two genes in MDA-MB-231 and MDA-MB-436 cells (**Fig. 5A, left**). This shows that two CpG sites in the TSS are highly methylated in MDA-MB-436 cells and comparably unmethylated in MDA-MB-231 cells (CpG sites 42064880 and 42064673). Accessing the breast cancer patient tumour data from TCGA revealed that methylation of these two CpG sites is highly negatively correlated with PLAT expression (**Fig. 5B**). Therefore, we conclude that the lack of PLAT/tPA expression in MDA-MB-436 cells is due to epigenetic silencing by DNA methylation of key CpGs in the TSS. This contrasts with the expression of PLAU/uPA in both MDA-MB-231 and MDA-MB-436 cells, which is well expressed and ALDH1A3 inducible, and as shown in **Fig. 5A (right**), PLAU has a similar CpG methylation profile in both cell lines. Assessment of the methylation levels of a couple of individual CpG methylation sites in the TSS and expression of PLAU in patient tumours did not reveal negative correlations with PLAU expression (**Fig. 5B, right**).

ALDH1A3's effects on breast cancer progression and gene expression have also been linked to its production of ATRA[69]. We therefore assessed for effects of ATRA on PLAT (tPA), PLAU (uPA), and SERPINB2 (PAI-2) in MDA-MB-231 cells. ATRA binds to nuclear hormone retinoic acid receptors (RARs), which dimerize with retinoid-X-receptors (RXRs) to induce expression of genes with retinoic acid response elements (RAREs) in their promoter sequence[35]. We performed a microarray analysis of RNA extracted from MDA-MB-231 cells treated with 100nM ATRA to evaluate gene expression changes in the presence of ATRA (**Fig 5C**). When examining the protease and protease regulator genes, PLAT was found to be significantly increased upon ATRA treatment. RT-qPCR confirmed increased PLAT expression upon ATRA treatment; however, unlike the gene expression effects induced by ALDH1A3 in MDA-MB-231 cells (**Fig. 1**), no significant changes were observed in SERBINB2 and PLAU (**Fig. 5D**). The ATRA regulation of PLAT is consistent with the observation that PLAT has a reported RARE sequence and tPA was induced by ATRA in human umbilical vein epithelial cells (HUVECs)[142,143].

Western blotting of cell lysates aligned with RT-qPCR and confirmed that ATRA increased intracellular tPA but did not affect uPA or PAI-2 levels (**Fig. 5E**). Consequently, ATRA treatment also increased secreted tPA and tPA activity (**Fig. 5F**). Cell surface plasmin activity was increased in ATRA-treated MDA-MB-231 cells (**Fig. 5G**). Overall, these results suggest that ATRA, which is made by ALDH1A3, is sufficient to induce PLAT/tPA and increase plasmin activity; however, ATRA and ALDH1A3 are not interchangeable and ALDH1A3 has ATRA-independent cell signalling effects not explained by ATRA production (e.g., effects on PLAU and SERPINB2 expression).

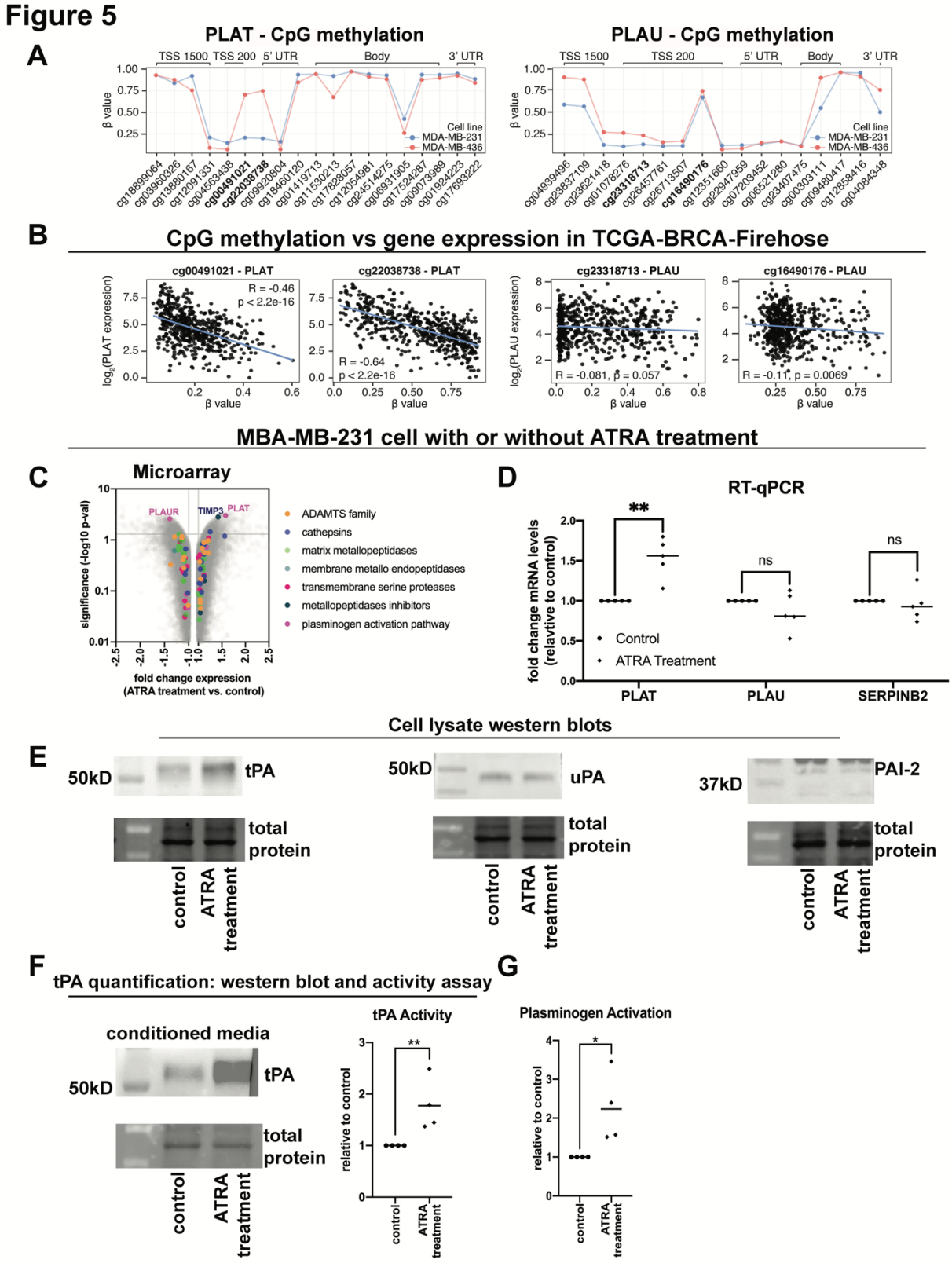

Figure 5. Methylation and ATRA affects the expression of PLAT and tPA activity in TNBC cells. (A) Illumina HumanMethylation450 (450K) beadchip array data of MDA-MB-231 and

MDA-MB-436 cell lines were obtained from GSE78875 project accessed through the NBCI Gene Expression Omnibus (GEO). β-values were obtained by processing the 450K data with the minfi R package. β-values for CpG sites within the regulatory and genic regions of PLAT (left panel) and PLAU (right panel) are shown. **(B)** RNA-sequencing expression versus methylation β-values of specific CpGs for PLAT and PLAU in breast cancer patient tumour samples from the TCGA Firehose cohort were obtained from the Broad Institute GDAC portal. CpG sites were selected based on data available from the 450K array and genomic localization. The Spearman coefficient (R) and corresponding p-value for the correlation between CpG methylation and gene expression are shown. **(C)** Transcriptome analysis of MDA-MB-231 cells (ATRA-treatment versus control cells) completed by Affymetrix Human Gene 2.0ST Array (n=3) identified differential expression of protease or protease regulator genes, the grey horizontal line indicates $p<0.05$. **(D)** RT-qPCR of MDA-MB-231 cells (no treatment control versus 100nM ATRA-treated cells) assesses for effects ATRA effects on expression of PLAT, PLAU, and SERPINB2 (n=5). **(E)** Western blots of cell lysates visually assessed for effects of ATRA treatment on tPA, uPA, and PAI-2 in MDA-MB-231 cell lysates (no treatment control versus 100nM ATRA-treated cell). **(F)** Western blots and tPA activity assays detect secreted tPA in conditioned media from MDA-MB-231 cells (no treatment control versus 100nM ATRA-treated cells, n=4). **(G)** The cell surface plasminogen activation assay was performed in MDA-MB-231 cells (no treatment control versus 100nM ATRA-treated cells, n=4). (**D, F, G**) Significance was determined by t-tests and significant p values are indicated as follows: * = <0.05, ** = <0.01 (ns = not significant).

3.5 ALDH1A3 and tPA proteins are co-expressed in breast cancer patient tumours

Having observed the regulation of plasmin activity and tPA/PLAT, uPA/PLAU, and PAI-2/SERPINB2 by ALDH1A3 in cultured TNBC cells along with positive gene expression correlations between ALDH1A3 and PLAT and PLAU in TNBC patient tumours (**Figs. 1-4**), we wondered if these correlations would be observed at the protein level in tumours.

We assessed a cohort of 78 archived fixed primary, treatment naïve, human breast tumour samples for co-expression between ALDH1A3 and tPA, uPA, and PAI-2 (**Table 3)**, tumour pathology and clinical details summarized). We include representative images of patient tumour sections stained with ALDH1A3 and tPA (**Fig. 6A**), ALDH1A3 and uPA (**Fig. 6B**), and ALDH1A3 and PAI-2 (**Fig. 6C**) and include examples of patient tumour samples that had low and high ALDH1A3 staining. Analysis of the patient samples revealed that ALDH1A3 staining was significantly and positively correlated with tPA staining, where ALDH1A3 and tPA were often co-expressed in the same cells (**Fig. 6A**). In contrast, ALDH1A3 staining was not positively correlated with uPA staining (**Fig. 6B**), nor negatively correlated with PAI-2 (**Fig. 6C**) as hypothesized. This data suggests that the *in vitro* regulation of plasminogen activation by ALDH1A3 is strongly reflected between ALDH1A3 and tPA in breast cancer patient tumours but not apparent between ALDH1A3 and uPA, or ALDH1A3 and PAI-2.

Figure 6

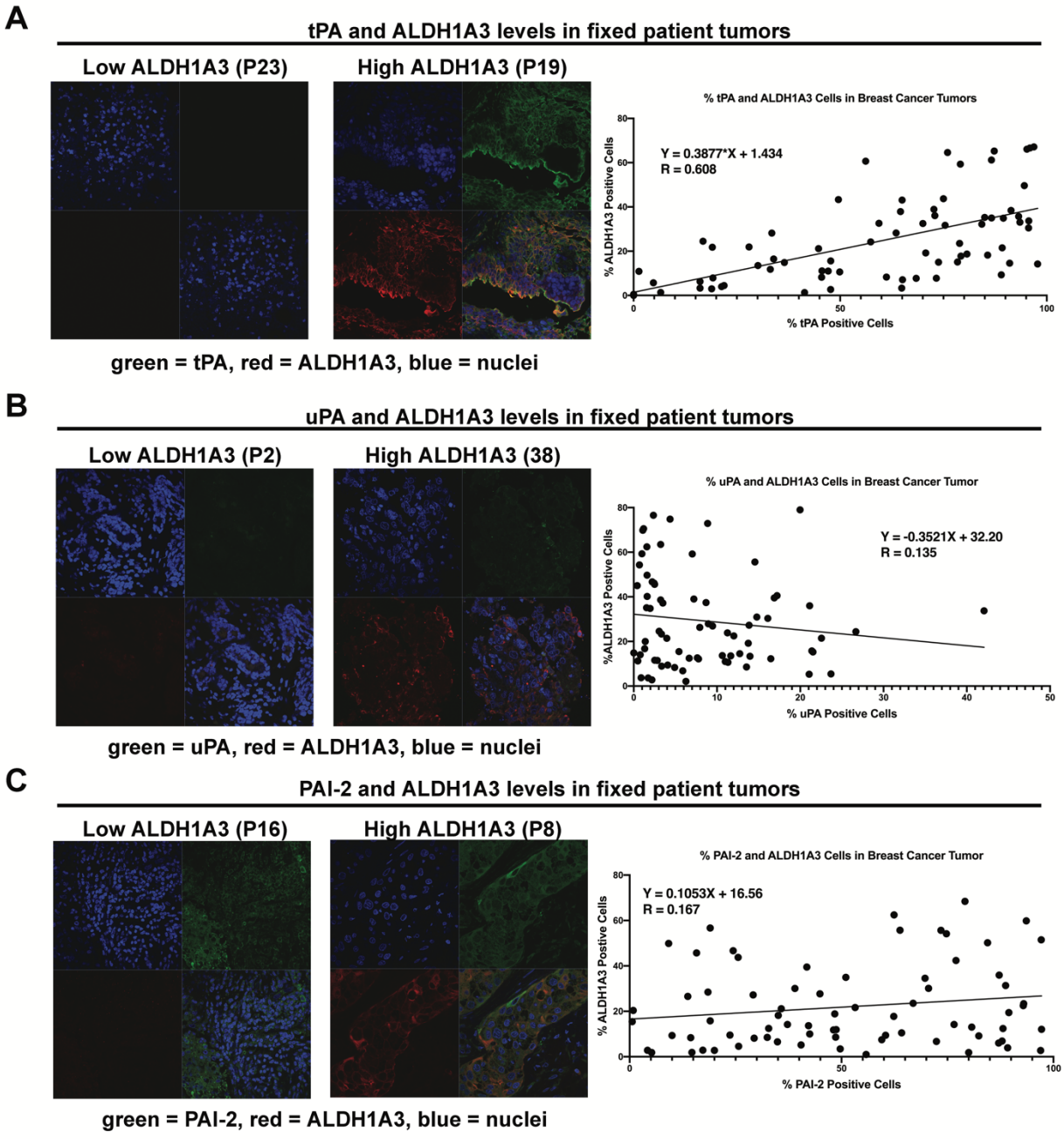

Figure 6. ALDH1A3 is co-expressed with tPA but not with uPA and PAI-2 in fixed breast cancer patient tumours. (**A-C**) Representative images of thin sections from a cohort of 78 formalin fixed paraffin-embedded patient tumour samples (patient number indicated in brackets, described in **Table 3**) were stained with antibodies specific to ALDH1A3 (red **A, B, and C**) and tPA (green, **A**), uPA (green, **B**), PAI-2 (green, **C**), and nuclei were stained with DAPI (blue) in the patient tumour samples. The graphs in **A**, **B**, **C** summarize the number of positive ALDH1A3 cells versus tPA **(A),** uPA **(B)** and PAI-2 **(C)** cells quantified by image J analysis of the stained thin sections from 73 fixed patient tumours. The number of positive cells in a patient tumour

sample was based on the average numbers from random images of at least three thin sections per tumour sample. Linear regression analysis of the graphs determined the co-expression correlation based on the slope and R value.

3.6 ALDH1A3 and tPA proteins are co-expressed in patient tumour cells and associated with TNBC subtype, high tumour grade, and worse progression-free survival

We analyzed for possible correlations between tumour pathology parameters and progression-free survival based on the percentage of positive ALDH1A3, tPA, uPA, and PAI-2 cells, or the combination of ALDH1A3 with tPA or uPA, or ALDH1A3 combined with PAI-2 negative cells. We assessed for associations with tumour stage, tumour grade, subtype, and lymph node involvement. We noted significant associations between high numbers of ALDH1A3+ and tPA+ cells and the TNBC subtype (non-TNBC versus TNBC) and higher tumour grade (grade 1 and 2 versus grade 3, **Fig. 7A**). We did not observe any significant correlations with other tumour pathology parameters (**Fig. 8A and B**; TMN stage and lymph node involvement). Whether we segregated patients based on individual lymph node involvement (yes/no), or lymph node stage (N0, N1, N2, N3) we did not obtain any significant correlations with ALDH1A3, tPA or uPA (**Fig. 8C**). The few patient tumour samples that had high levels of lymph node involvement (i.e., N2 or N3) limited the power of the analysis. Although we did not detect significant correlations, there were some trends with patients in the N2 or N3 groups having higher levels of tPA and uPA staining.

Next, we determined if having high (top 50% of tumours) versus low (bottom 50% of tumours) percentages of positive ALDH1A3, tPA, uPA, and PAI-2 cells, or having combined high ALDH1A3 and tPA (ALDH1A3+/tPA+) versus low ALDH1A3-/tPA-, high ALDH1A3 and uPA (ALDH1A3+/uPA+) versus low ALDH1A3-/uPA-, high ALDH1A3 and low PAI-2 (ALDH1A3+/PAI-2-) versus low ALDH1A3 and high PAI-2 (ALDH1A3-/PAI-2+) cells in patient tumours is associated with later disease progression. This revealed that ALDH1A3+ cells (HR= 2.389 log rank p= 0.0358) had the strongest association with disease progression, followed by the combination of ALDH1A3+/tPA+ cells (HR= 2.047 log rank p= 0.1196), and tPA+ alone

(HR= 1.210 log rank p= 0.64), while uPA+ and PAI-2- was weakly associated disease-free progression (trend, not significant) (**Fig. 7B**). Pairing ALDH1A3 with uPA or PAI-2 abrogated the association of ALDH1A3 with progression.

Overall, the staining of fixed breast cancer patient tumours suggests that among these four proteins, ALDH1A3 has the strongest associations with the TNBC subtype, higher tumour grade, and later recurrence (progression) and that tPA has similar associations that overlap with ALDH1A3. The lack of increased significant correlation with worse progression survival, when we assessed the combination of ALDH1A3+/tPA+ cells, could be due to the reduced number of patients analyzed when a double positive/double negative analysis was performed (total patients = 48, **Fig. 7B**) versus the greater patients when the single ALDH1A3+ stain analysis was performed (total patients = 69, **Fig. 7B).** The progression-free survival analysis also suggests that tPA alone is not a strong predictor of worse progression-free survival and that having tPA alone is not sufficient to promote later metastasis/recurrence. ALDH1A3 effects on metastasis development were strongly associated with worse progression-free survival as ALDH1A3 likely has other mechanisms to meditate metastasis, beyond tPA. Regardless, the observed significant co-expression of ALDH1A3 with tPA (**Fig. 7A**) suggests that when ALDH1A3 is expressed in a patient tumour, tPA is most likely present.

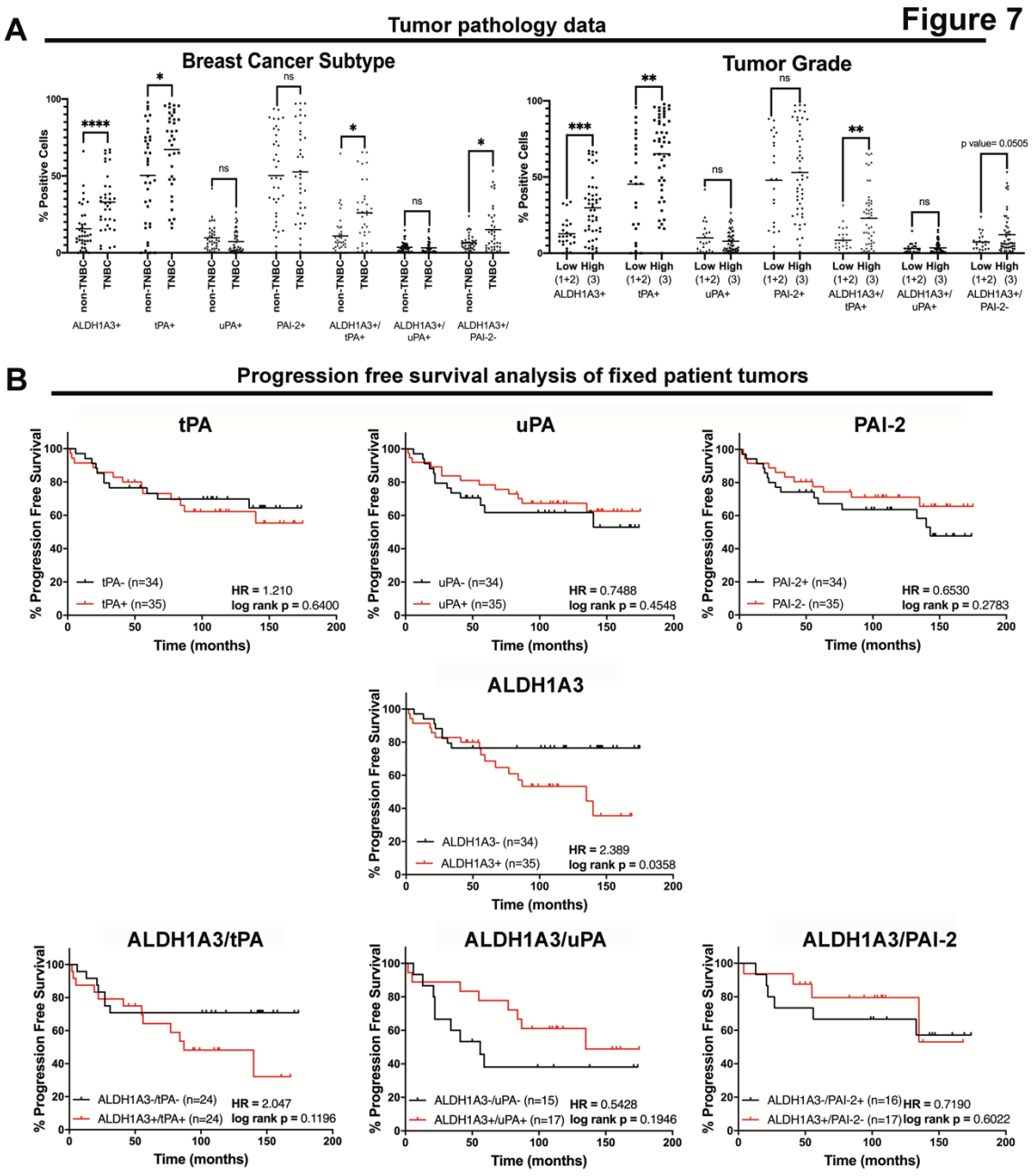

Figure 7. ALDH1A3 and tPA protein levels, but not uPA and PAI-2, are associated with the TNBC subtype, high tumour grade, and worse progression-free survival. (A) The panel of 78 formalin-fixed paraffin-embedded patient tumour samples (details of patient samples are provided in **Table 3**) are stained for ALDH1A3, tPA, uPA, and PAI-2 in the tumour samples in **Fig. 5** and quantified for positive and negative cells were divided into two groups based on breast cancer subtype (top left graph, non-TNBC = ER+/PR+ and HER+) and tumour grade (top right graph, low = grade 1 and 2, high = grade 3). **(B)** Kaplan-Meier progression-free survival analysis of the 73 breast cancer patient tumour cohort based on median number of ALDH1A3, tPA, uPA and PAI-2 positive cells or ALDH1A3 in combination with tPA, uPA, and PAI-2. HR = Hazard ratio; p = significance of log-rank test of survival probability.

Figure 8

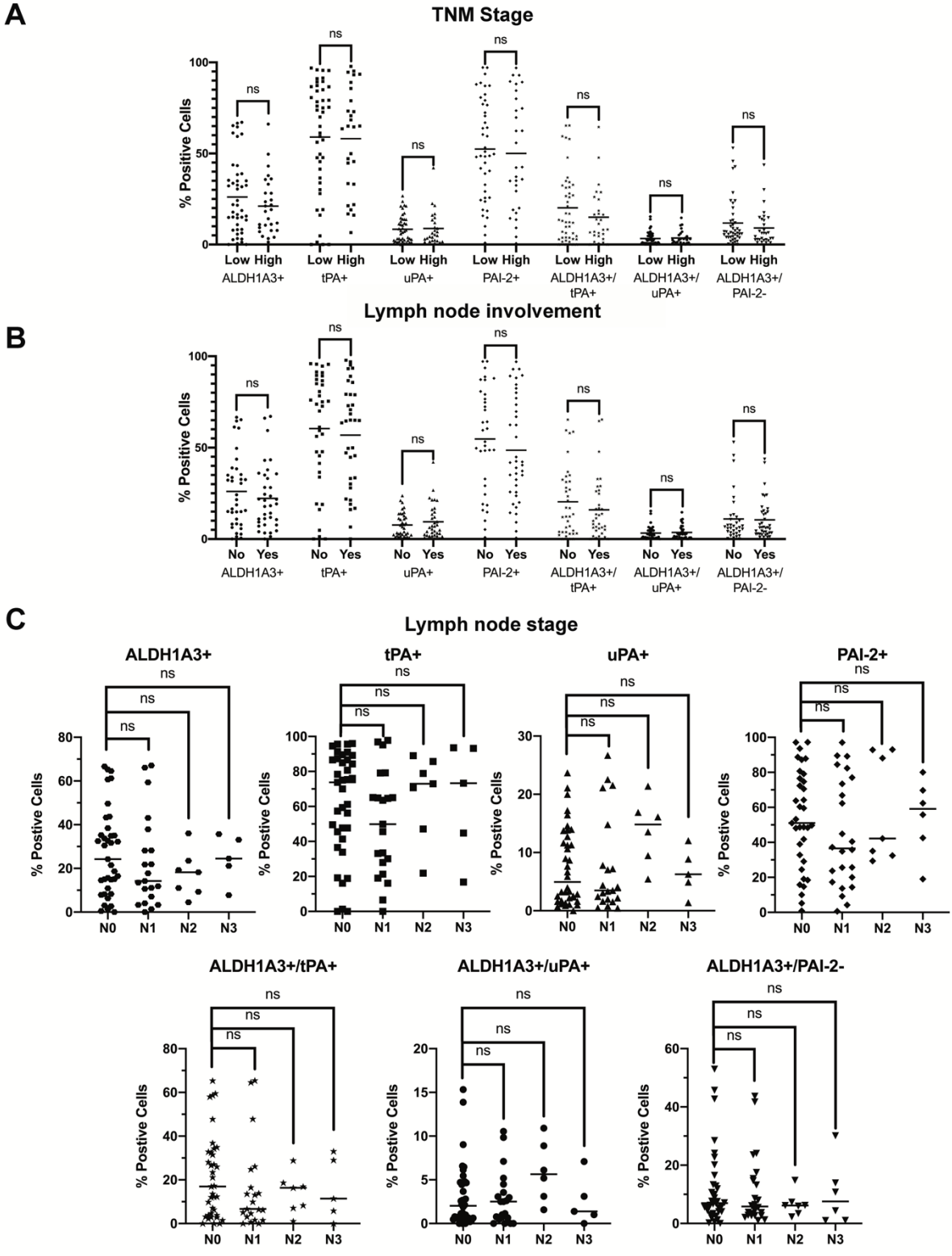

Figure 8. ALDH1A3, tPA, uPA and PAI-2 do not correlate with tumour stage or lymph node involvement. (A , B, C) A panel of formalin-fixed paraffin-embedded 78 breast cancer

patient tumour samples (described in **Table 3**) are stained for ALDH1A3, tPA, uPA, and PAI-2 for 73 samples and divided into two groups based on **(A)** TNM stage (Low = I, II, IIA stage; High = IIB, IIIA, IIIB, IIIC, IV stage) and **(B)** the presence of lymph node metastasis (no = N0 lymph node stage, yes = N1, N2 or N3 lymph node stage). **(C)** The patients are divided based on lymph node stage: N0, N1, N2 and N3 and the line represents the median. Significance was determined by one-way ANOVA followed by multiple comparison tests for experiments, ns = not significant.

3.7 tPA mediates plasmin activity, invasion, and increases lymph node metastasis of MDA-MB-231 cells

Having shown that in TNBC, ALDH1A3 regulates the plasminogen activation pathway, depends upon plasminogen for invasion, and among the plasminogen activation pathway factors is most strongly associated with PLAT/tPA, we next wondered if tPA affects plasmin activity, invasion, and TNBC tumour growth and metastasis. We therefore knocked down PLAT in MDA-MB-231 cells, with or without ALDH1A3 overexpression, by transient siRNA expression confirmed that this reduced PLAT/tPA and tPA activity in the TNBC cells (**Fig. 9A**). SiRNA Knockdown of PLAT/tPA reduced plasmin generation (**Fig. 10A**) and invasion (**Fig. 10B**) in vector control and ALDH1A3 overexpressing cells.

To examine the relationship between tPA and tumour progression *in vivo*, we generated stable knockdown of PLAT/tPA (**Fig. 9B**) in MDA-MB-231 cells and these cells had reduced tPA activity (**Fig. 9B**) and had reduced plasmin and invasion activity (**Fig. 10C and D**). We orthotopically implanted these MDA-MB-231 cells in immunocompromised female NOD/SCID mice and measured tumour growth and metastasis to the lymph nodes and lungs. Knockdown of tPA resulted in a significant decrease in tumour volume; however, at termination, the harvested tumours were not significantly smaller (**Fig. 10E**). We examined the mice at termination and noted visual differences in the axillary and inguinal lymph nodes, where some mice had noticeably enlarged axillary and/or inguinal lymph nodes indicative of metastatic disease (**Fig. 10F**). We collected the axillary and inguinal lymph nodes from each mouse and weighed the lymph nodes. This revealed a significantly lower total lymph node weight in mice that had been implanted with MDA-MB-231 cells with reduced tPA expression by knockdown (**Fig. 10G**). We confirmed that the enlarged lymph nodes consisted of predominately metastatic MDA-MB-231 cells by staining the fixed lymph nodes sections with H&E and anti-pan-cytokeratin antibody (stains epithelial cell

specifically, (**Fig. 10H; Fig. 11A)**, full images of node sections). As a negative control, we include analysis of lymph nodes harvested from a naïve mouse that had not been implanted with MDA-MB-231 cells (**bottom images, Fig. 10H**). The epithelial cells were absent in the lymph nodes of the negative control naïve mouse.

Finally, we examined the lungs for metastasis. We quantified the number of disseminated MDA-MB-231 cells using an RT-qPCR-based method which can accurately quantify between 10^2 – 10^6 MDA-MB-231 cells in the lung lobe of a mouse[132]. This revealed evidence of lung metastasis (**Fig. 10I**), which we confirmed by H&E (**Fig. 10J, Fig. 11B)**, full images of lung lobe sections). Although not significant, we observed a trend in reduced cancer cells in the lungs of mice implanted with MDA-MB-231 cells with reduced tPA expression by knockdown (**Fig. 10I**). Together these analyses suggest that reduced tPA in MDA-MB-231 cells impedes the early-stage of metastatic dissemination (i.e., to the lymph nodes); however, tPA reduction alone is not sufficient to significantly reduce overall metastasis as seen in the analysis of the lungs.

Figure 9

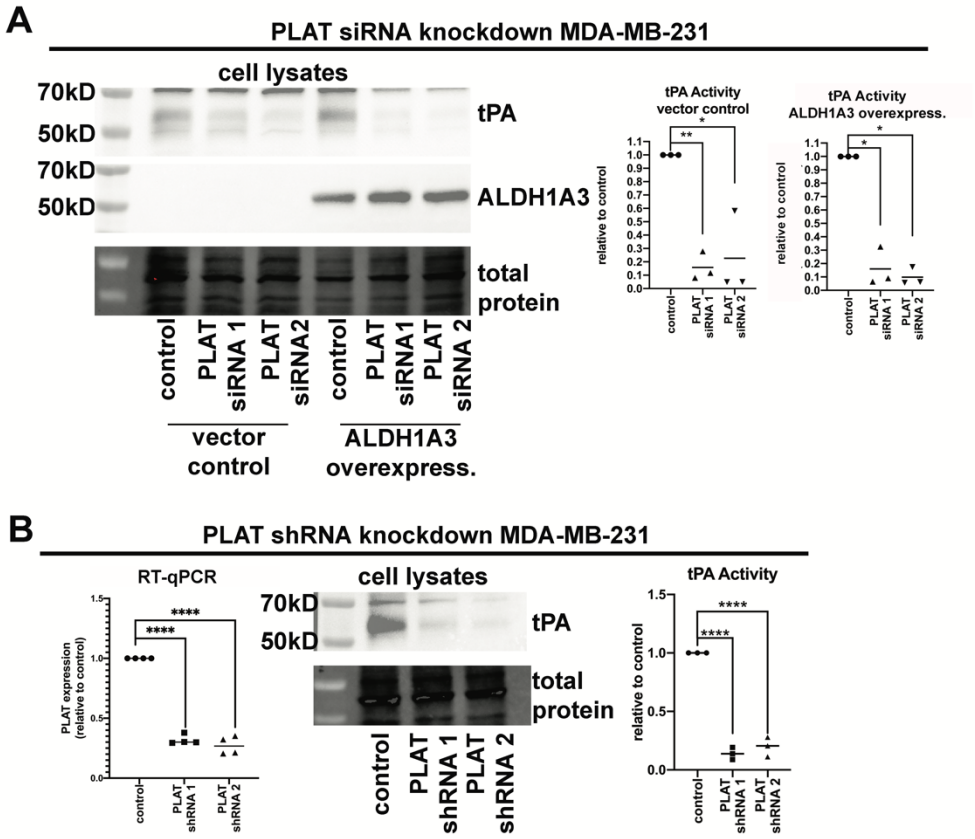

Figure 9. Generated PLAT knockdown in MDA-MB-231 cells reduced plasmin and tPA activity. (A) Western blot confirms PLAT siRNA in vector control and ALDH1A3 overexpressing cells MDA-MB-231 cells. tPA activity assays detect secreted tPA in conditioned media from MDA-MB-231 cells (siRNA control versus PLAT siRNA 1 and 2 are compared). **(B)** RT-qPCR and western blots confirmed PLAT/tPA knockdown in MDA-MB-231. (**C**) tPA activity assays detect secreted tPA in conditioned media from MDA-MB-231 cells (scramble shRNA control versus PLAT shRNA 1 and 2 are compared). (**A, B and C**) Significance was determined through one-way ANOVA followed by multiple comparisons analysis (n=3,4). Significant p values are indicated as follows: *** = <0.001, **** = <0.0001.

Figure 10

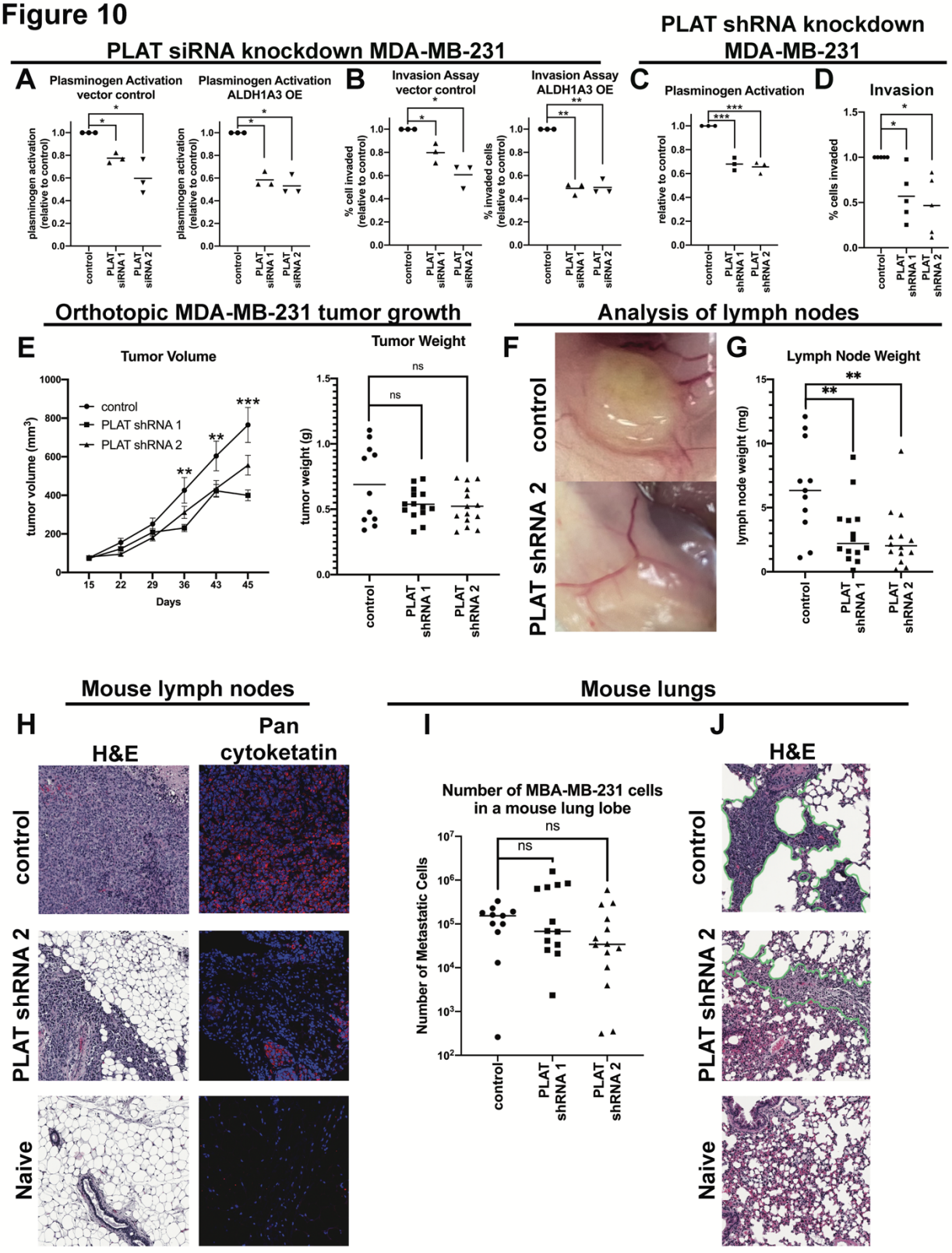

Figure 10. tPA knockdown reduces plasmin and invasion mediated by ALDH1A3 and lymph node metastasis of MDA-MB-231 cells orthotopically implanted in NOD/SCID mice.

(A, B) The cell surface plasminogen activation assay (**A**) or transwell invasion assay (**B**) was performed in MDA-MB-231 cells with or without ALDH1A3 overexpression treated with PLAT siRNA1 and 2. (C, D) The cell surface plasminogen activation assay (**C**) or transwell invasion assay (**D**) was performed in MDA-MB-231 cells with shRNA PLAT knockdown. (**A, B, C, and D**) Significance determined by one-way ANOVA followed by multiple comparison (**E)** Tumour volume and weights of mice injected with MDA-MB-231 shRNA scramble control, PLAT shRNA 1, and PLAT shRNA 2. Significance was determined through a one-way ANOVA followed by multiple comparison (n=11,15 and 15 respectively). **(F, G)** Representative images (**F**) and total lymph node weights (**G**, axillary and inguinal nodes combined per mouse) of mice from **E**. **(H)** Representative cropped images of H&E (10 x zoom of the scanned image of full node section, **Fig. 11**) and pan cytokeratin staining of the lymph nodes. **(I, J)** Analysis of mouse lungs from **E**. (**I**) Quantification of MDA-MB-231 cells (control versus shRNA 1 or 2) present in lung lobes of each mouse by RT-qPCR using human-specific GAPDH primers (the horizontal line indicates the median). Analysis for significance was determined by a one-way ANOVA, followed by multiple comparisons (n=11,15 and 15 respectively). (**J**) Representative cropped images of H&E (10 x zoom of scanned image of full lung lobe section, **Fig. 11**). Areas of metastatic cells are indicated with a green line.

Figure 11

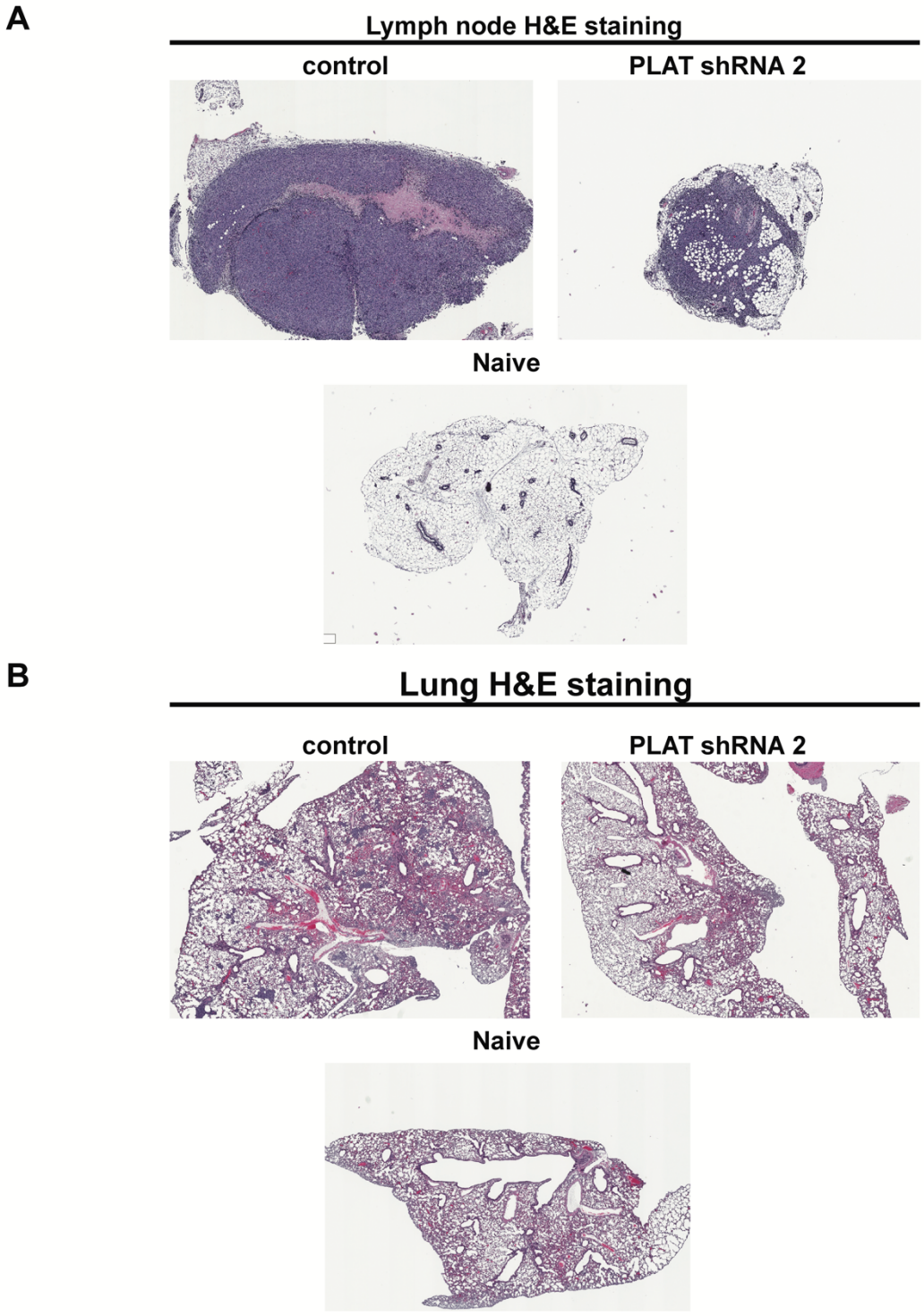

Figure 11. The full scanned H&E-stained images. Cropped images from Fig. 7 of the H&E-stained thin sections of the formalin fixed paraffin embedded lymph nodes and lungs from mice

implanted with MDA-MB-231 cells (control and PLAT knockdown) or negative control naïve mouse not implanted with cells. The scanned images were taken at 20x magnification.

Chapter 4 Discussion

4.1 ALDH1A3 is linked to poor patient survival and disease progression

ALDH1A3 has been shown to correlate with poor patient survival, disease progression, and recurrence in many cancers, including breast, prostate, glioblastoma, neuroblastoma, pancreatic, gastric, gall bladder, colon, and intrahepatic cholangiocarcinoma cancers[60,65,69–76]. Investigations into the function of ALDH1A3 in cancer suggest it promotes disease progression by both increasing tumour burden and metastasis[61,63,65,69,76]. Given that metastasis is the primary cause of cancer mortality it is critical to characterize pathways and factors that promote metastasis and therefore focus our investigation on understanding ALDH1A3-mediated invasion and metastasis.

Previous studies have linked ALDH1A3-mediated cancer progression to gene expression changes and ATRA[61,69,144], effects on epithelial-mesenchymal-transition[65,69,83], and altered glucose and GABA metabolism[62,145], however, the specific factors that mediate ALDH1A3 invasion and metastasis are largely unidentified. We, therefore, performed analyses to specifically identify factors that mediate the early stage of metastasis; the proteases and regulators of proteases that mediate cancer cell invasion through the remodelling of the extracellular matrix.

4.2 ALDH1A3 regulates important plasminogen activation players in TNBC cell lines and patient samples

Our analyses of TNBC show that ALDH1A3 transcriptionally regulates the plasminogen activation pathway, resulting in increased activity of the serine protease plasmin, which we link to ALDH1A3-mediated invasion. Specifically, in TNBC cells we find that ALDH1A3 can transcriptionally regulate PLAT, PLAU, and SERPINB2. In doing this, ALDH1A3 increases the expression of PLAT and PLAU while decreasing the expression of PAI-2 allowing for increased

levels of tPA and uPA to be secreted out of the cell. Conditioned media western blotting along with tPA and uPA activity assays shows that overexpression and knockdown of ALDH1A3 in different TNBC cell lines influences their secreted expression (**Figure 3**). This in turn directly correlates with plasmin levels. When ALDH1A3 was overexpressed in MDA-MB-231 cells, tPA, uPA and plasmin levels were all increased. Importantly, when knocking down tPA by siRNA's and shRNA's, plasmin levels were decreased (**Figure 10**). This shows that ALDH1A3 can regulate important plasminogen activation players to contribute to ECM degradation and cellular invasion. However, considering both the cell line and patient tumour data, the strongest overall evidence was between ALDH1A3 and PLAT/tPA.

In 73 patient tumours, ALDH1A3 was stained with either tPA, uPA or PAI-2 to examine co-expression levels. Overall, ALDH1A3 had the strongest correlation with tPA. Tumours that had ALDH1A3+/tPA+ cells also showed a positive association with the TNBC subtype, higher-grade tumours, and worse progression-free survival. When examining the co-expression of ALDH1A3 with uPA and PAI-2, we did not see any trends despite our cell line data. This may be attributed to the low number of TNBC patients stained in our study. Our cell line data was completed on TNBC cells. Out of the 73 patient samples we stained, only 36 were TNBC patients. To obtain a better understanding of uPA and PAI-2 in correlation with ALDH1A3 in TNBC, more staining will need to be conducted. Additionally, others have shown that high blood uPA is an independent predictor of metastatic breast cancer progression[146]. PAI-2 has been reported to be associated with progression-free survival and good outcomes[147]; we report a similar trend that is consistent with those previous reports. The lack of significance in our study could be explained by the smaller patient cohort we assessed.

Overall, our data was able to show a strong correlation between ALDH1A3, tPA and plasminogen activation. Importantly, changes in ALDH1A3 levels influenced the levels of plasminogen activation which led to ALDH1A3-plasmin-mediated cell invasion. We were able to show the important plasminogen activation plays that ALDH1A3 influences contribute to TNBC metastasis.

4.3 ALDH1A3 regulates PLAT through retinoic acid

It is noteworthy that in our gene expression analyses of PLAT, PLAU, and SERPINB2, we also found that PLAT was inducible by the nuclear hormone receptor ligand ATRA but PLAU and SERPINB2 were not. Notably, among PLAT, PLAU, and SERPINB2, only PLAT has been described to have a RARE, which is inducible ATRA[142,143]. Uchida et al., also showed that ATRA increased tPA activity and *in vitro* invasion in human oral squamous-cell-carcinoma lines [148]. Considering our current data showing that tPA promotes metastasis of MDA-MB-231 cells and is inducible by ATRA, it also partly explains our prior findings where like ALDH1A3, ATRA increased metastasis of MDA-MB-231 tumours[69]. In contrast to ATRA-inducible PLAT/tPA, other ALDH1A3-downstream co-regulatory mechanisms could be at play in the regulation of at least PLAU and SERPINB2, beyond the production of ATRA by ALDH1A3. In this context, ATRA-mediated induction of uPA in endothelial cells absent a RARE sequence has been described, where ATRA induces expression of RARs and RAR:RXRs heterodimers interact with Sp1 which ultimately leads to the transcription of uPA[149]. This reveals the dependence on other factors, which may be cell line or patient tumour-specific factors that may be less commonly expressed. For example, it has been previously described that ALDH1A3 regulates gene expression via microRNAs[74], long non-coding RNAs[150–155], and activation of the

phosphatidylinositol 3-kinase/Protein kinase B/rapamycin (PI3K/AKT/mTOR) signalling pathway[156]. It is possible that these ALDH1A3-regulated factors are contributing to the regulation of PLAU and SERPINB2 by ALDH1A3 and ATRA does not fully replicate the cell signalling events induced by ALDH1A3.

4.4 tPA plays an important role in the plasminogen activation pathway

The plasminogen activator tPA plays a physiologically important role in fibrinolysis and clot dissolution due to its function in plasminogen activation[157]. Several studies have also suggested a potential role of tPA in cancer progression based on expression and associations in patient tumours and blood samples. In 2005, Corte et. al., performed ELISA assays on homogenized tumour extracts from breast cancer patients to quantify cytosolic tumour tPA levels and noted that in only the subgroup of patients with lymph node-negative disease, tPA was associated with better overall survival; no correlations were found in other patient subgroups[158]. Other studies have investigated associations between cancer progression and serum levels of tPA (not in tumours). For example, low plasma/serum level of tPA was associated with poor disease-free survival and enhanced risk of breast cancer progression[159]. While, in other studies, higher levels of plasma tPA are linked to a greater risk of breast cancer and aggressive disease[160–162]. Although the above-mentioned studies indicate tPA as a biomarker of progressive (or non-progressive) breast cancer, an evaluation of the functional role of the protein upon knockdown or overexpression in cancer cells was lacking.

Our current study is the first one to examine the function of tPA expressed by cancer cells in tumour growth and metastasis using an orthotopic xenograft breast tumour mouse model. Although tPA knockdown did not significantly reduce lung metastatic burden, it did reduce lymph

node metastatic burden. Several factors could contribute to the lack of consistency between lymph node involvement in the patients and tPA knockdown observed in the mouse model employed here. First, the patient tumours are more complex and heterogeneous, which can differentially influence the lymph node involvement, including the expedited timeline from initial tumour formation in the mouse model to metastasis, which occurs in a matter of weeks in the tumour xenograft model but could take years in humans. Furthermore, the lack of a functional adaptive immune system in our mouse tumour mode could alter the metastatic trajectory of the cells in comparison to humans. Overall, these data suggest tPA contributes to the metastatic trajectory of breast cancer cells but tPA reduction is not sufficient to inhibit lung metastasis. Notably, plasmin activation is mediated by multiple factors in addition to tPA (e.g., uPA); therefore, tPA knockdown alone only partially reduces plasmin activity. Residual plasmin activity generated by uPA could be sufficient to mediate lung metastasis despite the reduced lymph node metastasis we observed.

4.5 Limitations and further directions

In this study, we have determined that ALDH1A3 plays a role in secreting tPA and uPA out of the cell to increase plasminogen activation. However, the mechanisms behind tPA and uPA secretion to the extracellular matrix from cancer cells remains unclear. Rontogianni et al completed a proteomic analysis on MBA-MB-231 extracellular vesicles and found the presence of tPA and uPA within the vesicles[163]. Therefore, we hypothesise that ALDH1A3 may be increasing tPA and uPA secretion through vesicle secretion. To test this hypothesis, extracellular vesicles can be isolated from conditioned media from cells with or without ALDH1A3 expression. These isolated extracellular vesicles will be assessed for tPA and uPA levels by western blotting.

A major limitation that we faced was creating a cell line that simultaneously overexpressed ALDH1A3 and knocked down PLAT. Although we were able to see the effects of PLAT knockdown in MDA-MB-231 cells, these cells naturally have very low levels of ALDH1A3. Therefore, in the mouse experiment, we were only studying the effects of tPA. Unfortunately, we are unable to successfully select stable PLAT shRNA lentiviral knockdown clones in a clone already selected for stable overexpression by ALDH1A3. Despite this, we still performed transient PLAT siRNA knockdown in ALDH1A3 overexpressing MDA-MB-231 cells in vitro.

Finally, Breast cancer is a complex, heterogeneous disease, where the tumour-host interface plays an important role in cancer progression[164]. Single gene knockdown studies in mouse models can only provide a limited understanding of the complex multidimensional disease of cancer. Future studies with ALDH1A3 and tPA-plasmin axis link will/should investigate in the context of the complexity of the tumour ecological system.

Chapter 5 Conclusions

In summary, our analyses suggest a novel mechanism of ALDH1A3-mediated invasion and metastasis in TNBC via the regulation of the plasminogen activation pathway. This pathway has multiple players and levels of regulation, and our evidence strongly links ALDH1A3 with tPA in TNBC. ALDH1A3 is an important player in the progression of several other cancers, hence it will be crucial to evaluate if ALDH1A3 regulates the plasminogen activation pathway in these cancers as well. It is also clear from our analyses and the review of the literature that ALDH1A3 has multi-factorial effects in cancer progression which is unlikely to be explained by a single gene or protein. Therefore, strategies that target ALDH1A3 specifically may remain the best way to ensure therapeutic effects are broadly applicable.

References

1 Sudhakar A. History of Cancer, Ancient and Modern Treatment Methods. https://doi.org/10.4172/1948-5956.100000e2.

2 Faguet GB. A brief history of cancer: Age-old milestones underlying our current knowledge database. *Int J Cancer*. 2015;**136**(9):2022–2036.

3 Haggard HW, Smith GM. JOHANNES MULLER AND THE MODERN CONCEPTION OF CANCER*. *YALB JOURNAL OF BIOLOGY AND MEDICINE*.**10**(5).

4 Bujalkova M, Lan- F. Hippocrates' humoral pathology in nowaday's reflections. *Bratisl Lek Listy*. 2001;**102**(10):489–492.

5 The Discovery of the Double Helix, 1951-1953 | Francis Crick - Profiles in Science. https://profiles.nlm.nih.gov/spotlight/sc/feature/doublehelix. Accessed 26 August 2023.

6 Torry DS, Cooper GM. Proto-Oncogenes in Development and Cancer. *American Journal of Reproductive Immunology*. 1991;**25**(3):129–132.

7 Macleod K. Tumor suppressor genes. *Curr Opin Genet Dev*. 2000;**10**(1):81–93.

8 Reunanen N, Kähäri V. Matrix Metalloproteinases in Cancer Cell Invasion. 2013.

9 Pezzoli D, Di Paolo J, Kumra H, Fois G, Candiani G, Reinhardt DP, et al. Fibronectin promotes elastin deposition, elasticity and mechanical strength in cellularised collagen-based scaffolds. *Biomaterials*. 2018;**180**:130–142.

10 Westermarck J, Ka¨ha¨ri V-M, Ka¨ha K, Ka¨ha¨ri K. Regulation of matrix metalloproteinase expression in tumor invasion. *The FASEB Journal*. 1999;**13**(8):781–792.

11 Cairns R, Khokha R, Hill R. Molecular Mechanisms of Tumor Invasion and Metastasis: An Integrated View. *Curr Mol Med*. 2005;**3**(7):659–671.

12 Gheldof A, Berx G. Cadherins and Epithelial-to-Mesenchymal Transition. *Prog Mol Biol Transl Sci*. 2013;**116**:317–336.

13 Shiozaki H, Oka H, Inoue M, Tamura S, Monden M. E-cadherin Mediated Adhesion System in Cancer Cells. 1995. https://doi.org/10.1002/(SICI)1097-0142(19960415)77:8.

14 Lyon B, Lyon F, Mehlen P, Puisieux A. Metastasis: a question of life or death. *Nat Rev Cancer*. 2006;**6**:449.

15 Brenner D, Poirier A, Demers A, Ellison L, Finley C, Fitzgerald N, et al. Members of the Canadian Cancer Statistics Advisory Committee Project management. 2022.

16 Makki J. Diversity of Breast Carcinoma: Histological Subtypes and Clinical Relevance. *Clin Med Insights Pathol*. 2015;**8**(1):23.

17 Eheman CR, Shaw KM, Ryerson AB, Miller JW, Ajani UA, White MC. The changing incidence of in situ and invasive ductal and lobular breast carcinomas: United States, 1999-2004. *Cancer Epidemiology Biomarkers and Prevention*. 2009;**18**(6):1763–1769.

18 Orrantia-Borunda E, Anchondo-Nuñez P, Acuña-Aguilar LE, Gómez-Valles FO, Ramírez-Valdespino CA. Subtypes of Breast Cancer. *Breast Cancer*. 2022;31–42.

19 Waks AG, Winer EP. Breast Cancer Treatment: A Review. *JAMA*. 2019;**321**(3):288–300.

20 Osborne CK. Tamoxifen in the Treatment of Breast Cancer. *https://doi.org/101056/NEJM199811263392207*. 1998;**339**(22):1609–1618.

21 Jahanzeb M. Adjuvant Trastuzumab Therapy for HER2-Positive Breast Cancer. *Clin Breast Cancer*. 2008;**8**(4):324–333.

22 Wein L, Loi S. Mechanisms of resistance of chemotherapy in early-stage triple negative breast cancer (TNBC). *The Breast*. 2017;**34**:S27–S30.

23 Ensenyat-Mendez M, Llinàs-Arias P, Orozco JIJ, Íñiguez-Muñoz S, Salomon MP, Sesé B, et al. Current Triple-Negative Breast Cancer Subtypes: Dissecting the Most Aggressive Form of Breast Cancer. *Front Oncol*. 2021;**11**:681476.

24 Zagami P, Carey LA. Triple negative breast cancer: Pitfalls and progress. *npj Breast Cancer 2022 8:1*. 2022;**8**(1):1–10.

25 Hsu LC, Chang WC, Hiraoka L, Hsieh CL. Molecular cloning, genomic organization, and chromosomal localization of an additional human aldehyde dehydrogenase gene, ALDH6. *Genomics*. 1994;**24**(0888-7543 (Print)):333–341.

26 Koppaka V, Thompson DC, Chen Y, Ellermann M, Nicolaou KC, Juvonen RO, et al. Aldehyde dehydrogenase inhibitors: a comprehensive review of the pharmacology, mechanism of action, substrate specificity, and clinical application. *Pharmacol Rev*. 2012;**64**(3):520–539.

27 Marchitti SA, Brocker C, Stagos D, Vasiliou V. Non-P450 aldehyde oxidizing enzymes: the aldehyde dehydrogenase superfamily. *Expert Opin Drug Metab Toxicol*. 2008;**4**(6):697–720.

28 Li H, Wagner E, McCaffery P, Smith D, Andreadis A, Dräger UC. A retinoic acid synthesizing enzyme in ventral retina and telencephalon of the embryonic mouse. *Mech Dev*. 2000;**95**(1–2):283–289.

29 Mic FA, Molotkov A, Fan X, Cuenca AE, Duester G. RALDH3, a retinaldehyde dehydrogenase that generates retinoic acid, is expressed in the ventral retina, otic vesicle and olfactory pit during mouse development. *Mech Dev*. 2000;**97**(1–2):227–230.

30 Yahyavi M, Abouzeid H, Gawdat G, de Preux AS, Xiao T, Bardakjian T, et al. ALDH1A3 loss of function causes bilateral anophthalmia/microphthalmia and hypoplasia of the optic nerve and optic chiasm. *Hum Mol Genet*. 2013;**22**(16):3250.

31 Molotkova N, Molotkov A, Duester G. Role of retinoic acid during forebrain development begins late when Raldh3 generates retinoic acid in the ventral subventricular zone. *Dev Biol*. 2007;**303**(2):601–610.

32 Sima A, Parisotto M, Mader S, Bhat P V. Kinetic characterization of recombinant mouse retinal dehydrogenase types 3 and 4 for retinal substrates. *BiochimBiophysActa*. 2009;**1790**(0006-3002 (Print)):1660–1664.

33 D Z, P M, KJ I, RL N, P H, WW C, et al. Molecular identification of a major retinoic-acid-synthesizing enzyme, a retinaldehyde-specific dehydrogenase. 1996;**240**(1):15–22.

34 Black W, Vasiliou V. The Aldehyde Dehydrogenase Gene Superfamily Resource Center. *Hum Genomics*. 2009;**4**(2):136.

35 Coyle KM, Sultan M, Thomas ML, Vaghar-Kashani A, Marcato P, Mohammad Sultan KMC. Retinoid Signaling in Cancer and Its Promise for Therapy. *J Carcinog Mutagen*. 2013;0–14.

36 Cunningham TJ, Duester G. Mechanisms of retinoic acid signalling and its roles in organ and limb development. *Nature Reviews Molecular Cell Biology 2015 16:2*. 2015;**16**(2):110–123.

37 Lalevee S, Anno YN, Chatagnon A, Samarut E, Poch O, Laudet V, et al. Genome-wide in silico identification of new conserved and functional retinoic acid receptor response elements (direct repeats separated by 5 bp). *J BiolChem*. 2011;**286**(1083–351X (Electronic)):33322–33334.

38 Arteaga MF, Mikesch J-H, Fung T-K, So CWE. Epigenetics in acute promyelocytic leukaemia pathogenesis and treatment response: a TRAnsition to targeted therapies. *Br J Cancer*. 2015;**112**(3):413–418.

39 Yoshida H, Kitamura K, Tanaka K, Omura S, Miyazaki T, Hachiya T, et al. Accelerated degradation of PML-retinoic acid receptor alpha (PML-RARA) oncoprotein by all-trans-retinoic acid in acute promyelocytic leukemia: possible role of the proteasome pathway. *Cancer Res*. 1996;**56**(13):2945–2948.

40 Ablain J, De Th E H. Retinoic acid signaling in cancer: The parable of acute promyelocytic leukemia. https://doi.org/10.1002/ijc.29081.

41 Chen F, Shao F, Hinds A, Yao S, Ram-Mohan S, Norman TA, et al. Retinoic acid signaling is essential for airway smooth muscle homeostasis. *JCI Insight*. 2018;**3**(16).

42 Defnet AE, Shah SD, Huang W, Shapiro P, Deshpande DA, Kane MA. Dysregulated retinoic acid signaling in airway smooth muscle cells in asthma. *The FASEB Journal*. 2021;**35**(12):e22016.

43 Chen F, Marquez H, Kim YK, Qian J, Shao F, Fine A, et al. Prenatal retinoid deficiency leads to airway hyperresponsiveness in adult mice. *J Clin Invest*. 2014;**124**(2):801–811.

44 Clagett-Dame M, Knutson D. Vitamin A in Reproduction and Development. *Nutrients 2011, Vol 3, Pages 385-428*. 2011;**3**(4):385–428.

45 Hao M, Zan J. The Identification of Childhood Asthma Progression-Related lncRNAs and mRNAs Suitable as Biomarkers Using Weighted Gene Coexpression Network Analysis. *Genet Res (Camb)*. 2021;**2021**.

46 Murar M, Vaidya A. Cancer stem cell markers: premises and prospects. *http://dx.doi.org/102217/bmm1585*. 2015;**9**(12):1331–1342.

47 Marcato P, Dean CA, Giacomantonio CA, Lee PWK. Aldehyde dehydrogenase its role as a cancer stem cell marker comes down to the specific isoform. Cell Cycle. 2011;**10**(9):1378–1384.

48 Ginestier C, Hur MH, Charafe-Jauffret E, Monville F, Dutcher J, Brown M, et al. ALDH1 Is a Marker of Normal and Malignant Human Mammary Stem Cells and a Predictor of Poor Clinical Outcome. *Cell Stem Cell*. 2007;**1**(1934-5909 (Electronic)):555–567.

49 Cheung AM, Wan TS, Leung JC, Chan LY, Huang H, Kwong YL, et al. Aldehyde dehydrogenase activity in leukemic blasts defines a subgroup of acute myeloid leukemia with adverse prognosis and superior NOD/SCID engrafting potential. *Leukemia*. 2007;**21**(0887-6924 (Print)):1423–1430.

50 Ma S, Chan KW, Lee TK, Tang KH, Wo JY, Zheng BJ, et al. Aldehyde dehydrogenase discriminates the CD133 liver cancer stem cell populations. *MolCancer Res*. 2008;**6**(1541-7786 (Print)):1146–1153.

51 Chen YC, Chen YW, Hsu HS, Tseng LM, Huang PI, Lu KH, et al. Aldehyde dehydrogenase 1 is a putative marker for cancer stem cells in head and neck squamous cancer. *Biochem Biophys Res Commun*. 2009;**385**(3):307–313.

52 Jiang F, Qiu Q, Khanna A, Todd NW, Deepak J, Xing L, et al. Aldehyde dehydrogenase 1 is a tumor stem cell-associated marker in lung cancer. *MolCancer Res*. 2009;**7**(1541-7786 (Print)):330–338.

53 Kim MP, Fleming JB, Wang H, Abbruzzese JL, Choi W, Kopetz S, et al. ALDH activity selectively defines an enhanced tumor-initiating cell population relative to CD133 expression in human pancreatic adenocarcinoma. *PLoS One*. 2011;**6**(6).

54 Rao QX, Yao TT, Zhang BZ, Lin RC, Chen ZL, Zhou H, et al. Expression and functional role of ALDH1 in cervical carcinoma cells. *Asian Pac J Cancer Prev*. 2012;**13**(4):1325–1331.

55 Todaro M, Iovino F, Eterno V, Cammareri P, Gambara G, Espina V, et al. Tumorigenic and metastatic activity of human thyroid cancer stem cells. *Cancer Res*. 2010;**70**(1538-7445 (Electronic)):8874–8885.

56 van den Hoogen C, Van der HG, Cheung H, Buijs JT, Lippitt JM, Guzman-Ramirez N, et al. High aldehyde dehydrogenase activity identifies tumor-initiating and metastasis-initiating cells in human prostate cancer. *Cancer Res*. 2010;**70**(1538-7445 (Electronic)):5163–5173.

57 Huang EH, Hynes MJ, Zhang T, Ginestier C, Dontu G, Appelman H, et al. Aldehyde dehydrogenase 1 is a marker for normal and malignant human colonic stem cells (SC) and tracks SC overpopulation during colon tumorigenesis. *Cancer Res*. 2009;**69**(1538-7445 (Electronic)):3382–3389.

58 Su Y, Qiu Q, Zhang X, Jiang Z, Leng Q, Liu Z, et al. Aldehyde dehydrogenase 1 A1-positive cell population is enriched in tumor-initiating cells and associated with progression of bladder cancer. *Cancer EpidemiolBiomarkers Prev*. 2010;**19**(1538-7755 (Electronic)):327–337.

59 Storms RW, Trujillo AP, Springer JB, Shah L, Colvin OM, Ludeman SM, et al. Isolation of primitive human hematopoietic progenitors on the basis of aldehyde dehydrogenase activity. *ProcNatlAcadSciUSA*. 1999;**96**(0027-8424 (Print)):9118–9123.

60 Marcato P, Dean CA, Da P, Araslanova R, Gillis M, Joshi M, et al. Aldehyde Dehydrogenase Activity of Breast Cancer Stem Cells Is Primarily Due To Isoform ALDH1A3 and Its Expression Is Predictive of Metastasis. *Stem Cells*. 2011;**29**(1):32–45.

61 Luo Y, Dallaglio K, Chen Y, Robinson WA, Robinson SE, McCarter MD, et al. ALDH1A Isozymes are Markers of Human Melanoma Stem Cells and Potential Therapeutic Targets. *Stem Cells*. 2012;**30**(1549-4918 (Electronic)):2100–2113.

62 Mao P, Joshi K, Li J, Kim SH, Li P, Santana-Santos L, et al. Mesenchymal glioma stem cells are maintained by activated glycolytic metabolism involving aldehyde dehydrogenase 1A3. *ProcNatlAcadSciUSA*. 2013;**110**(1091-6490 (Electronic)):8644–8649.

63 Shao C, Sullivan JP, Girard L, Augustyn A, Yenerall P, Rodriguez-Canales J, et al. Essential role of aldehyde dehydrogenase 1A3 for the maintenance of non-small cell lung

cancer stem cells is associated with the STAT3 pathway. *Clinical Cancer Research*. 2014;**20**(15):4154–4166.

64 Feng H, Liu YYY, Bian X, Zhou F, Liu YYY. ALDH1A3 affects colon cancer in vitro proliferation and invasion depending on CXCR4 status. *British Journal of Cancer 2018 118:2*. 2017;**118**(2):224–232.

65 Chen MHHHHH, Weng JJ, Cheng CT, Wu RC, Huang SC, Wu CE, et al. ALDH1A3, the major aldehyde dehydrogenase isoform in human cholangiocarcinoma cells, affects prognosis and gemcitabine resistance in cholangiocarcinoma patients. *Clinical Cancer Research*. 2016;**22**(16):4225–4235.

66 Kurth I, Hein L, Mäbert K, Peitzsch C, Koi L, Cojoc M, et al. Cancer stem cell related markers of radioresistance in head and neck squamous cell carcinoma. *Oncotarget*. 2015;**6**(33):34494–34509.

67 Lang T, Xu J, Zhou L, Zhang Z, Ma X, Gu J, et al. Disruption of KDM4C-ALDH1A3 feed-forward loop inhibits stemness, tumorigenesis and chemoresistance of gastric cancer stem cells. *Signal Transduction and Targeted Therapy 2021 6:1*. 2021;**6**(1):1–3.

68 Greve B, Kelsch R, Spaniol K, Eich HT, Götte M. Flow cytometry in cancer stem cell analysis and separation. *Cytometry A*. 2012;**81**(4):284–293.

69 Marcato P, Dean CA, Liu R-Z, Coyle KM, Bydoun M, Wallace M, et al. Aldehyde dehydrogenase 1A3 influences breast cancer progression via differential retinoic acid signaling. 2014. https://doi.org/10.1016/j.molonc.2014.07.010.

70 Wang S, Liang C, Bao M, Li X, Zhang L, Li S, et al. ALDH1A3 correlates with luminal phenotype in prostate cancer. *Tumour Biol*. 2017;**39**(4).

71 Gan C, Pierscianek D, Hindy N El, Ahmadipour Y, Keyvani K, Sure U, et al. The predominant expression of cancer stem cell marker ALDH1A3 in tumor infiltrative area is associated with shorter overall survival of human glioblastoma. https://doi.org/10.1186/s12885-020-07153-0.

72 Flahaut M, Jauquier N, Chevalier N, Nardou K, Balmas Bourloud K, Joseph J-M, et al. Aldehyde dehydrogenase activity plays a Key role in the aggressive phenotype of neuroblastoma. https://doi.org/10.1186/s12885-016-2820-1.

73 Yang ZL, Yang L, Zou Q, Yuan Y, Li J, Liang L, et al. Positive ALDH1A3 and negative GPX3 expressions are biomarkers for poor prognosis of gallbladder cancer. *Dis Markers*. 2013;**35**(3):163–172.

74 Duan JJ, Wang D, Cai J, Chen J jie, Zheng XX, Chen T qing, et al. An aldehyde dehydrogenase 1A3 inhibitor attenuates the metastasis of human colorectal cancer. *Cancer Lett*. 2022;**536**:215662.

75 Kawakami R, Mashima T, Kawata N, Kumagai K, Migita T, Sano T, et al. ALDH1A3-mTOR axis as a therapeutic target for anticancer drug-tolerant persister cells in gastric cancer. *Cancer Sci*. 2020;**111**(3):962–973.

76 Nie S, Qian X, Shi M, Li H, Peng C, Ding X, et al. ALDH1A3 Accelerates Pancreatic Cancer Metastasis by Promoting Glucose Metabolism. *Front Oncol*. 2020;**10**:915.

77 Kim YJ, Yoon HY, Kim JS, Kang HW, Min BD, Kim SK, et al. HOXA9, ISL1 and ALDH1A3 methylation patterns as prognostic markers for nonmuscle invasive bladder cancer: Array-based DNA methylation and expression profiling. *Int J Cancer*. 2013;**133**(5):1135–1142.

78 Ma YM, Zhao S. Prognostic values of aldehyde dehydrogenase 1 isoenzymes in ovarian cancer. *Onco Targets Ther*. 2016;**9**:1981–1988.

79 Samson JM, Ravindran Menon D, Smith DE, Baird E, Kitano T, Gao D, et al. Clinical implications of ALDH1A1 and ALDH1A3 mRNA expression in melanoma subtypes. *Chem Biol Interact*. 2019;**314**:108822.

80 Cheng M, Duan PG, Gao ZZ, Dai M. MicroRNA-487b-3p inhibits osteosarcoma chemoresistance and metastasis by targeting ALDH1A3. *Oncol Rep*. 2020;**44**(6):2691–2700.

81 Pérez-Alea M, Mcgrail K, Sánchez-Redondo S, Ferrer B, Fournet G, Cortés J, et al. ALDH1A3 is epigenetically regulated during melanocyte transformation and is a target for melanoma treatment. *Nature Publishing Group*. 2017;**36**:5695–5708.

82 Hua TNM, Namkung J, Phan ANH, Vo VTA, Kim MK, Jeong Y, et al. PPARgamma-mediated ALDH1A3 suppression exerts anti-proliferative effects in lung cancer by inducing lipid peroxidation. *https://doi.org/101080/1079989320181468781*. 2018;**38**(3):191–197.

83 Croker AK, Rodriguez-Torres M, Xia Y, Pardhan S, Sing Leong H, Lewis JD, et al. Differential Functional Roles of ALDH1A1 and ALDH1A3 in Mediating Metastatic Behavior and Therapy Resistance of Human Breast Cancer Cells. *International Journal of Molecular Sciences 2017, Vol 18, Page 2039*. 2017;**18**(10):2039.

84 Franken NAP, Rodermond HM, Stap J, Haveman J, van Bree C. Clonogenic assay of cells in vitro. *Nat Protoc*. 2006;**1**(5):2315–2319.

85 Thomas ML, de Antueno R, Coyle KM, Sultan M, Cruickshank BM, Giacomantonio MA, et al. Citral reduces breast tumor growth by inhibiting the cancer stem cell marker ALDH1A3. *Mol Oncol*. 2016;**10**(9):1485–1496.

86 Huang X, Hou Y, Weng X, Pang W, Hou L, Liang Y, et al. Oncogenesis Diethyldithiocarbamate-copper complex (CuET) inhibits colorectal cancer progression via

miR-16-5p and 15b-5p/ALDH1A3/PKM2 axis-mediated aerobic glycolysis pathway. 2021;**10**:4.

87 Koblinski JE, Ahram M, Sloane BF. Unraveling the role of proteases in cancer. *Clinica Chimica Acta*. 2000;**291**(2):113–135.

88 Rakashanda S, Rana F, Rafiq S, Masood A, Amin S. Role of proteases in cancer: A review. *Biotechnology and Molecular Biology Review*. 2012;**7**(4):90–101.

89 Quesada V, Ordóñez GR, Sánchez LM, Puente XS, López-Otín C. The Degradome database: mammalian proteases and diseases of proteolysis. *Nucleic Acids Res*. 2009;**37**(suppl_1):D239–D243.

90 Rocks N, Paulissen G, Hour M El, Quesada F, Crahay C, Gueders M, et al. Emerging roles of ADAM and ADAMTS metalloproteinases in cancer. 2007. https://doi.org/10.1016/j.biochi.2007.08.008.

91 McGowan PM, Ryan BM, Hill ADK, McDermott E, O'Higgins N, Duffy MJ. ADAM-17 Expression in Breast Cancer Correlates with Variables of Tumor Progression. *Clinical Cancer Research*. 2007;**13**(8):2335–2343.

92 Cal S, López-Otín C. ADAMTS proteases and cancer. *Matrix Biology*. 2015;**44–46**:77–85.

93 Choi SY, Bertram S, Glowacka I, Park YW, Pöhlmann S. Type II transmembrane serine proteases in cancer and viral infections. *Trends Mol Med*. 2009;**15**(7):303–312.

94 Tomlins SA, Rhodes DR, Perner S, Dhanasekaran SM, Mehra R, Sun XW, et al. Recurrent fusion of TMPRSS2 and ETS transcription factor genes in prostate cancer. *Science (1979)*. 2005;**310**(5748):644–648.

95 He Y, Liu X-D, Chen Z-Y, Zhu J, Xiong Y, Li K, et al. Interaction between Cancer Cells and Stromal Fibroblasts Is Required forActivation of the uPAR-uPA-MMP-2 Cascade in Pancreatic Cancer Metastasis. https://doi.org/10.1158/1078-0432.CCR-06-2088.

96 Andreasen PA, Egelund R, Petersen HH. The plasminogen activation system in tumor growth, invasion, and metastasis. 2000;**57**(1):25–40.

97 Davis GE, Pintar Allen KA, Salazar R, Maxwell SA. Matrix metalloproteinase-1 and -9 activation by plasmin regulates a novel endothelial cell-mediated mechanism of collagen gel contraction and capillary tube regression in three-dimensional collagen matrices. *J Cell Sci*. 2001;**114**(Pt 5):917–930.

98 Lijnen HR. Molecular interactions between the plasminogen/plasmin and matrix metalloproteinase systems. *Fibrinolysis and Proteolysis*. 2000;**14**(2–3):175–181.

99 Saksela O. Plasminogen activation and regulation of pericellular proteolysis. *Biochim Biophys Acta*. 1985;**823**(1):35–65.

100 Kwaan HC, Weiss I, Tallman MS. The Role of Abnormal Hemostasis and Fibrinolysis in Morbidity and Mortality of Acute Promyelocytic Leukemia. *Semin Thromb Hemost*. 2019;**45**(6):612–621.

101 Christensen LR. STREPTOCOCCAL FIBRINOLYSIS: A PROTEOLYTIC REACTION DUE TO A SERUM ENZYME ACTIVATED BY STREPTOCOCCAL FIBRINOLYSIN. *J Gen Physiol*. 1945;**28**(4):363–383.

102 Kwaan HC, McMahon B. The role of plasminogen-plasmin system in cancer. *Cancer Treat Res*. 2009;**148**:43–66.

103 Andronicos NM, Ranson M. The topology of plasminogen binding and activation on the surface of human breast cancer cells. *Br J Cancer*. 2001;**85**(6):909–916.

104 Miles L, Parmer R. Plasminogen receptors: the first quarter century. *Semin Thromb Hemost*. 2013;**39**(4):329–337.

105 Ranson M, Andronicos NM, O'Mullane MJ, Baker MS. Increased plasminogen binding is associated with metastatic breast cancer cells: differential expression of plasminogen binding proteins. *Br J Cancer*. 1998;**77**(10):1586–1597.

106 Stillfried GE, Saunders DN, Ranson M. Plasminogen binding and activation at the breast cancer cell surface: the integral role of urokinase activity. *Breast Cancer Res*. 2007;**9**(1).

107 Danø K, Andreasen PA, Grøndahl-Hansen J, Kristensen P, Nielsen LS, Skriver L. Plasminogen activators, tissue degradation, and cancer. *Adv Cancer Res*. 1985;**44**(C):139–266.

108 Wiman B, Collen D. Molecular mechanism of physiological fibrinolysis. *Nature 1978 272:5653*. 1978;**272**(5653):549–550.

109 Sharma M, Ownbey RT, Sharma MC. Breast cancer cell surface annexin II induces cell migration and neoangiogenesis via tPA dependent plasmin generation Overexpression of annexin II in cancer seems to correlate with advanced stage with poor prognosis and. *Exp Mol Pathol*. 2009;**88**:278–286.

110 Holst-Hansen C, Johannessen B, Hoyer-Hansen G, Romer J, Ellis V, Briinner N. Urokinase-type plasminogen activation in three human breast cancer cell lines correlates with their in vitro invasiveness. *Clin Exp Metastasis*. 1996;**14**:297–307.

111 Whitley BR, Palmieri D, Twerdi CD, Church FC. Expression of active plasminogen activator inhibitor-1 reduces cell migration and invasion in breast and gynecological cancer cells. *Exp Cell Res*. 2004;**296**(2):151–162.

112 Balsara RD, Ploplis VA. Plasminogen activator inhibitor-1: The double-edged sword in apoptosis. *Thromb Haemost*. 2008;**100**(6):1029–1036.

113 Koumarianou A, Karayannopoulou G, Gourgioti G, Batistatou A, Bobos M, Efstratiou I, et al. PAI-1 and HER2 interaction in advanced breast cancer disease: evidence for added benefit from trastuzumab in HER2-negative patients. *Cancer Chemother Pharmacol*. 2015;**75**:1289–1301.

114 Li C, Cao S, Liu Z, Ye X, Chen L, Meng S. RNAi-mediated downregulation of uPAR synergizes with targeting of HER2 through the ERK pathway in breast cancer cells. *Int J Cancer*. 2010;**127**(7):1507–1516.

115 Eatemadi A, Aiyelabegan HT, Negahdari B, Mazlomi MA, Daraee H, Daraee N, et al. Role of protease and protease inhibitors in cancer pathogenesis and treatment. 2016. https://doi.org/10.1016/j.biopha.2016.12.021.

116 Hosono H, Ohishi T, Takei J, Asano T, Sayama Y, Kawada M, et al. The anti-epithelial cell adhesion molecule (EpCAM) monoclonal antibody EpMab-16 exerts antitumor activity in a mouse model of colorectal adenocarcinoma. *Oncol Lett*. 2020;**20**(6):1–1.

117 Desai A, Yan Y, Gerson SL. Concise Reviews: Cancer Stem Cell Targeted Therapies: Toward Clinical Success. *Stem Cells Transl Med*. 2019;**8**(1):75–81.

118 Ghanbari-Movahed M, Ghanbari-Movahed Z, Momtaz S, Kilpatrick KL, Farzaei MH, Bishayee A. Unlocking the Secrets of Cancer Stem Cells with γ-Secretase Inhibitors: A Novel Anticancer Strategy. *Molecules*. 2021;**26**(4).

119 Brown JM, Wasson MCD, Marcato P. The Missing Lnc: The Potential of Targeting Triple-Negative Breast Cancer and Cancer Stem Cells by Inhibiting Long Non-Coding RNAs. *Cells 2020, Vol 9, Page 763*. 2020;**9**(3):763.

120 Pal A, Pattanayak RD, Sagar R. Tracing the journey of disulfiram: From an unintended discovery to a treatment option for alcoholism. *Journal of Mental Health and Human Behaviour*. 2015;**20**(1):41.

121 Kannappan V, Ali M, Small B, Rajendran G, Elzhenni S, Taj H, et al. Recent Advances in Repurposing Disulfiram and Disulfiram Derivatives as Copper-Dependent Anticancer Agents. *Front Mol Biosci*. 2021;**8**.

122 Lin J, Haffner MC, Zhang Y, Lee BH, Brennen WN, Britton J, et al. Disulfiram is a DNA demethylating agent and inhibits prostate cancer cell growth. *Prostate*. 2011;**71**(4):333–343.

123 R. Kona F, Buac D, M. Burger A. Disulfiram, and disulfiram derivatives as novel potential anticancer drugs targeting the ubiquitin-proteasome system in both preclinical and clinical studies. *Curr Cancer Drug Targets*. 2011;**11**(3):338–346.

124 Zirjacks L, Stransky N, Klumpp L, Prause L, Eckert F, Zips D, et al. Repurposing Disulfiram for Targeting of Glioblastoma Stem Cells: An In Vitro Study. *Biomolecules*. 2021;**11**(11).

125 Cheng P, Wang J, Waghmare I, Sartini S, Coviello V, Zhang Z, et al. FOXD1-ALDH1A3 signaling is a determinant for the self-renewal and tumorigenicity of mesenchymal glioma stem cells. *Cancer Res*. 2016;**76**(24):7219–7230.

126 Yamashita D, Minata M, Ibrahim AN, Yamaguchi S, Coviello V, Bernstock JD, et al. Identification of ALDH1A3 as a viable therapeutic target in breast cancer metastasis-initiating cells. *Mol Cancer Ther*. 2020;**19**(5):1134–1147.

127 Gelardi ELM, Colombo G, Picarazzi F, Ferraris DM, Mangione A, Petrarolo G, et al. A Selective Competitive Inhibitor of Aldehyde Dehydrogenase 1A3 Hinders Cancer Cell Growth, Invasiveness and Stemness In Vitro. *Cancers (Basel)*. 2021;**13**(2):1–20.

128 Kamiyama H, Miyano M, Ito D, Kimura T, Hagiwara K, Kogai H, et al. Identification of a novel ALDH1A3-selective inhibitor by a chemical probe with unrelated bioactivity: An approach to affinity-based drug target discovery. *Chem Biol Drug Des*. 2022. https://doi.org/10.1111/CBDD.14176.

129 Moretti A, Li J, Donini S, Sobol RW, Rizzi M, Garavaglia S. Crystal structure of human aldehyde dehydrogenase 1A3 complexed with NAD+ and retinoic acid. *Scientific Reports 2016 6:1*. 2016;**6**(1):1–12.

130 Li J, Garavaglia S, Ye Z, Moretti A, Belyaeva O V, Beiser A, et al. A specific inhibitor of ALDH1A3 regulates retinoic acid biosynthesis in glioma stem cells. *Communications Biology 2021 4:1*. 2021;**4**(1):1–16.

131 Zhang F, Guo J, Zhang Z, Qian Y, Wang G, Duan M, et al. Mesenchymal stem cell-derived exosome: A tumor regulator and carrier for targeted tumor therapy. *Cancer Lett*. 2022;**526**:29–40.

132 Dahn ML, Dean CA, Jo DB, Coyle KM, Marcato P. Human-specific GAPDH qRT-PCR is an accurate and sensitive method of xenograft metastasis quantification. *Mol Ther Methods Clin Dev*. 2021;**20**:398–408.

133 Cerami E, Gao J, Dogrusoz U, Gross BE, Sumer SO, Aksoy BA, et al. The cBio cancer genomics portal: an open platform for exploring multidimensional cancer genomics data. *Cancer Discov*. 2012;**2**(5):401–404.

134 Gao J, Aksoy BA, Dogrusoz U, Dresdner G, Gross B, Sumer SO, et al. Integrative analysis of complex cancer genomics and clinical profiles using the cBioPortal. *Sci Signal*. 2013;**6**(269).

135 Su CW, Lin CW, Yang WE, Yang SF. TIMP-3 as a therapeutic target for cancer. *Ther Adv Med Oncol*. 2019;**11**.

136 Fan D, Kassiri Z. Biology of Tissue Inhibitor of Metalloproteinase 3 (TIMP3), and Its Therapeutic Implications in Cardiovascular Pathology. *Front Physiol*. 2020;**11**:661.

137 Keragala CB, Medcalf RL. Plasminogen: an enigmatic zymogen. *Blood*. 2021;**137**(21):2881–2889.

138 Croucher DR, Saunders DN, Lobov S, Ranson M. Revisiting the biological roles of PAI2 (SERPINB2) in cancer. *Nat Rev Cancer*. 2008;**8**(7):535–545.

139 Westrick RJ, Røjkjær LP, Yang AY, Roh MH, Siebert AE, Ginsburg D. Deficiency of plasminogen activator inhibitor-2 results in accelerated tumor growth. *J Thromb Haemost*. 2020;**18**(11):2968–2975.

140 Steinberg J, Ritchie GRS, Roumeliotis TI, Jayasuriya RL, Clark MJ, Brooks RA, et al. Integrative epigenomics, transcriptomics and proteomics of patient chondrocytes reveal genes and pathways involved in osteoarthritis. *Scientific Reports 2017 7:1*. 2017;**7**(1):1–11.

141 Coyle KM, Murphy JP, Vidovic D, Vaghar-Kashani A, Dean CA, Sultan M, et al. Breast cancer subtype dictates DNA methylation and ALDH1A3-mediated expression of tumor suppressor RARRES1. *Oncotarget*. 2016;**7**(28):44096.

142 Medh RD, Santell L, Levin EG. Stimulation of Tissue Plasminogen Activator Production by Retinoic Acid: Synergistic Effect on Protein Kinase C-Mediated Activation. *Blood*. 1992;**80**(4):981.

143 Balmer JE, Blomhoff R. Gene expression regulation by retinoic acid. *J Lipid Res*. 2002;**43**(11):1773–1808.

144 Sullivan KE, Rojas K, Cerione RA, Nakano I, Wilson KF. The stem cell/cancer stem cell marker ALDH1A3 regulates the expression of the survival factor tissue transglutaminase, in mesenchymal glioma stem cells. *Oncotarget*. 2017;**8**(14):22325–22343.

145 Dahn ML, Walsh HR, Dean CA, Giacomantonio MA, Fernando W, Murphy JP, et al. Metabolite profiling reveals a connection between aldehyde dehydrogenase 1A3 and GABA metabolism in breast cancer metastasis. *Metabolomics*. 2022;**18**(1).

146 Banys-Paluchowski M, Witzel I, Aktas B, Fasching PA, Hartkopf A, Janni W, et al. The prognostic relevance of urokinase-type plasminogen activator (uPA) in the blood of patients with metastatic breast cancer. *Sci Rep*. 2019;**9**(1).

147 J A Foekens 1, F Buessecker, H A Peters, U Krainick, W L van Putten, M P Look, J G Klijn MDK. Plasminogen Activator Inhibitor-2: Prognostic Relevance in 1012 Patients with Primary Breast. Accessed 31 March 2023.

148 Uchida D, Kawamata H, Nakashiro K, Omotehara F, Hino S, Hoque MO, et al. Low-dose retinoic acid enhances in vitro invasiveness of human oral squamous-cell-carcinoma cell lines. *Br J Cancer*. 2001;**85**(1):122–128.

149 Suzuki Y, Shimada J, Shudo K, Matsumura M, Crippa MP, Kojima S. Physical Interaction Between Retinoic Acid Receptor and Sp1: Mechanism for Induction of Urokinase by Retinoic Acid. *Blood*. 1999;**93**(12):4264–4276.

150 Vidovic D, Huynh TT, Konda P, Dean C, Cruickshank BM, Sultan M, et al. ALDH1A3-regulated long non-coding RNA NRAD1 is a potential novel target for triple-negative breast tumors and cancer stem cells. *Cell Death Differ*. 2020;**27**(1):363–378.

151 Ke C, Shen M, Wang P, Chen Z, Lin S, Dong F. ALDH1A3-Linc00284 Axis Mediates the Invasion of Colorectal Cancer by Targeting TGF β Signaling via Sponging miR-361-5p. *Int J Genomics*. 2022;**2022**.

152 Yan D, Wu F, Peng C, Wang M. Silencing of LINC00284 inhibits cell proliferation and migration in oral squamous cell carcinoma by the miR-211-3p/MAFG axis and FUS/KAZN axis. *Cancer Biol Ther*. 2021;**22**(2):149–163.

153 Zhu M, Yan X, Zhao Y, Xue H, Wang Z, Wu B, et al. lncRNA LINC00284 promotes nucleus pulposus cell proliferation and ECM synthesis via regulation of the miR-205-3p/Wnt/β-catenin axis. *Mol Med Rep*. 2022;**25**(5).

154 Zhou B, Ge Y, Shao Q, Yang L, Chen X, Jiang G. Long noncoding RNA LINC00284 facilitates cell proliferation in papillary thyroid cancer via impairing miR-3127-5p targeted E2F7 suppression. *Cell Death Discov*. 2021;**7**(1).

155 You J, Li J, Ke C, Xiao Y, Lu C, Huang F, et al. Oncogenic long intervening noncoding RNA Linc00284 promotes c-Met expression by sponging miR-27a in colorectal cancer. *Oncogene*. 2021;**40**(24):4151–4166.

156 Yin H, Qin H, Yang L, Chen M, Yang Y, Zhang W, et al. circCYP24A1 promotes Docetaxel resistance in prostate Cancer by Upregulating ALDH1A3. *Biomark Res*. 2022;**10**(1).

157 Collen D, Lijnen HR. The tissue-type plasminogen activator story. *Arterioscler Thromb Vasc Biol*. 2009;**29**(8):1151–1155.

158 Corte MD, Vérez P, Rodríguez JC, Roibás A, Domínguez ML, Lamelas ML, et al. Tissue-type plasminogen activator (tPA) in breast cancer: relationship with clinicopathological parameters and prognostic significance. *Breast Cancer Res Treat*. 2005;**90**(1):33–40.

159 Wrzeszcz K, Słomka A, Zarychta E, Rhone P, Ruszkowska-Ciastek B. Tissue Plasminogen Activator as a Possible Indicator of Breast Cancer Relapse: A Preliminary,

Prospective Study. *Journal of Clinical Medicine 2022, Vol 11, Page 2398*. 2022;**11**(9):2398.

160 Ruszkowska-Ciastek B, Kwiatkowska K, Bielawska S, Robakowska M, Bielawski K, Rhone P. Evaluation of the prognostic value of fibrinolytic elements in invasive breast carcinoma patients. *Neoplasma*. 2020;**67**(5):1146–1156.

161 Costanzo S, Parisi R, De Curtis A, Gamba S, Russo L, Persichillo M, et al. Tissue Plasminogen Activator Levels and Risk of Breast Cancer in a Case-Cohort Study on Italian Women: Results from the Moli-sani Study. *Thromb Haemost*. 2021;**121**(4):449–456.

162 Chernicky CL, Yi L, Tan H, Ilan J. Tissue-type plasminogen activator is upregulated in metastatic breast cancer cells exposed to insulin-like growth factor-I. *Clin Breast Cancer*. 2005;**6**(4):340–348.

163 Rontogianni S, Synadaki E, Li B, Liefaard MC, Lips EH, Wesseling J, et al. Proteomic profiling of extracellular vesicles allows for human breast cancer subtyping. *Communications Biology 2019 2:1*. 2019;**2**(1):1–13.

164 Luo W. Nasopharyngeal carcinoma ecology theory: cancer as multidimensional spatiotemporal "unity of ecology and evolution" pathological ecosystem. *Theranostics*. 2023;**13**(5):1607–1631.

Appendix 1 Copyright permission

Introduction Sections 1.3-1.7 and 1.9

McLean ME, MacLean M, Cahill HF, Arun RP, Walker OL, Wasson MCD, Fernando W, Venkatesh J, Marcato P (2023) The expanding role of cancer stem cell marker ALDH1A3 in cancer and beyond, *Cancers*. DOI: 10.3390/cancers15020492

No special permission is required to reuse all or part of articles published by MDPI, including figures and tables. For articles published under an open access Creative Common CC BY license, any part of the article may be reused without permission provided that the original article is clearly cited. Reuse of an article does not imply endorsement by the authors or MDPI.

Appendix 2 Copyright permission

Chapters 2, 3 and 4

Bharadwaj A*, McLean ME*, Dahn ML*, Cahill HF, Wasson MCD, Pranap RA, Walker OA, Venkatesh J, Barnes PJ, Bethune G, Knapp G, Helyer L, Giacomantonio CA, Cruickshank BM, Waisman DM, Marcato PP (2023) ALDH1A3 promotes invasion and metastasis in triple-negative breast cancer by regulating the plasminogen activation pathway, *Molecular Oncology*. DOI: 10.1002/1878-0261.13528